2022

Effect of thiosulfate on the passivation of zinc-alloyed anodes, (Z32120 and Z13000) at 80°C after 288h immersion in 3.5% NaCl solution

Thwelt Thinzar Zaw
Faculty of Engineering

Effect of thiosulfate on the passivation of zinc-alloyed anodes, (Z32120 and Z13000) at 80°C after 288h immersion in 3.5% NaCl solution

Miss Thwelt Thinzar Zaw

A Thesis Submitted in Partial Fulfillment of the Requirements
for the Degree of Master of Engineering in Metallurgical and Materials Engineering
Department of Metallurgical Engineering
FACULTY OF ENGINEERING
Chulalongkorn University
Academic Year 2022

ผลของไธโอซัลเฟตต่อการเกิดพาสซิเวชันของโลหะผสมสังกะสี (Z32120 และ Z13000) หลังจากแช่อยู่ในสารละลายเกลือโซเดียมคลอไรด์ 3.5% นาน 288 ชั่วโมง ที่ 80 องศาเซลเซียส

น.ส.เท็ต ทินซา ซอว์

วิทยานิพนธ์นี้เป็นส่วนหนึ่งของการศึกษาตามหลักสูตรปริญญาวิศวกรรมศาสตรมหาบัณฑิต
สาขาวิชาวิศวกรรมโลหการและวัสดุ ภาควิชาวิศวกรรมโลหการ
คณะวิศวกรรมศาสตร์ จุฬาลงกรณ์มหาวิทยาลัย
ปีการศึกษา 2565

Thesis Title	Effect of thiosulfate on the passivation of zinc-alloyed anodes, (Z32120 and Z13000) at 80°C after 288h immersion in 3.5% NaCl solution
By	Miss Thwelt Thinzar Zaw
Field of Study	Metallurgical and Materials Engineering
Thesis Advisor	Professor Dr. GOBBOON LOTHONGKUM, Ing.

Accepted by the FACULTY OF ENGINEERING, Chulalongkorn University in Partial Fulfillment of the Requirement for the Master of Engineering

..... Dean of the FACULTY OF ENGINEERING
(Professor SUPOT TEACHAVORASINSKUN, D.Eng.)

THESIS COMMITTEE

..... Chairman
(Assistant Professor Dr. PANYAWAT WANGYAO, Ph.D)

..... Thesis Advisor
(Professor Dr. GOBBOON LOTHONGKUM, Ing.)

..... Examiner
(Dr. NITHI SAENARJHAN, Ph.D.)

..... External Examiner
(Dr. Wanida Pongsaksawad, Ph.D.)

เท็ต ทินซา ซอว์ : ผลของไธโอซัลเฟตต่อการเกิดพาสซิเวชันของโลหะผสมสังกะสี (Z32120 และ Z13000) หลังจากแช่อยู่ในสารละลายเกลือโซเดียมคลอไรด์ 3.5% นาน 288 ชั่วโมง ที่ 80 องศาเซลเซียส. (Effect of thiosulfate on the passivation of zinc-alloyed anodes, (Z32120 and Z13000) at 80°C after 288h immersion in 3.5% NaCl solution) อ.ที่ปรึกษาหลัก : กอบบุญ หล่อทองคำ

ในงานวิจัยนี้ศึกษาการขัดขวางการเกิดฟิล์มพาสซีฟของ โลหะผสมสังกะสี (Z32120 และZ13000) ในน้ำทะเลเทียมอณหภูมิ 80 องศาเซลเซียส ที่ผสมไธโอซัลเฟตเข้มข้น100 150 200 พีพีเอ็ม ด้วยวิธีการทางไฟฟ้าเคมี หลังจากจุ่มแช่นาน 288 ชั่วโมง และเปรียบเทียบผลลับกรณีที่ไม่ผสมไธโอซัลเฟต ผลการทดลองพบว่า ไธโอซัลเฟตขัดขวางการเกิดฟิล์มพาสซีฟที่เกิดขึ้นจาการจุ่มแช่ในน้ำทะเลเทียมที่ไม่ผสมโอซัลเฟต ระหว่าง 120 และ 288 ชั่วโมง ไธโอซัลเฟตส่งเสริมการซึมของไอออนคลอไรด์ (Cl^-) ไม่เพียงแต่ขัดขวางการเกิดฟิล์มพาสซีฟแต่ส่งเสริมการทำลายฟิล์มพาสซีฟด้วยผลรวมจึงเป็นการขัดขวางการเกิดฟิล์มพาสซีฟ ผลการทดลองยืนยันจากการเปรียบเทียบกราฟโพลาไรเซชันของกรณีผสมและไม่ผสมไธโอซัลเฟต แม้ว่าไธโอซัลเฟตขัดขวางการเกิดฟิล์มพาสซีฟแต่ความแตกต่างความเข้มข้นให้ประสิทธิผลต่างกัน ประสิทธิผลขึ้นอยู่กับเวลาการจุ่มแช่และอุณหภูมิ อะลูมิเนียมผสมในโลหะมีผลต่อประสิทธิผลด้วยเช่นกัน ความเข้มข้นไธโอซัลเฟตต่ำกว่า (100 พีพีเอ็ม) ให้ผลการลดลงของความหนาแน่นกระแสที่เวลาจุ่มแช่นานกว่าสำหรับ Z32120 สำหรับ Z13000 ห้ผลการลดลงของความหนาแน่นกระแสที่ความเข้มข้นไธโอซัลเฟต 200 พีพีเอ็ม จากผลการทดลอง Z32120 เกิดประสิทธิผล ที่ไธโอซัลเฟตเข้มข้น 150 และ 200 พีพีเอ็ม Z1300 เกิดประสิทธิผลดีกว่าที่ไธโอซัลเฟตเข้มข้น 100 และ 150 พีพีเอ็ม ดังนั้นที่ไธโอซัลเฟตเข้มข้น 150 พีพีเอ็ม คือปริมาณเหมาะสมสำหรับโลหะผสมทั้งสองชนิด ผลของไธโอของซัลเฟตต่อการเกิดฟิล์มพาสซีฟของโลหะทั้งสองได้วิเคราะห์พิจารณาถึงเวลาการจุ่มแช่ อุณหภูมิ ความเป็นกรดด่าง และสัดส่วนของ ไอออนคลอไรด์ต่อไอออนซัลเฟต

สาขาวิชา	วิศวกรรมโลหการและวัสดุ	ลายมือชื่อนิสิต .....
ปีการศึกษา	2565	ลายมือชื่อ อ.ที่ปรึกษาหลัก .....

6272043221 : MAJOR METALLURGICAL AND MATERIALS ENGINEERING
KEYWORD: Thiosulfate, Zinc alloyed anodes, Polarization, Passivation, Depassivation

Thwelt Thinzar Zaw : Effect of thiosulfate on the passivation of zinc-alloyed anodes, (Z32120 and Z13000) at 80°C after 288h immersion in 3.5% NaCl solution. Advisor: Prof. Dr.-Ing. GOBBOON LOTHONGKUM, Ing.

In this research, the inhibition of passivation on Zn alloys (Z32120 with Al) and Z13000 without Al) in artificial seawater (3.5% NaCl) mixing with different thiosulfate concentrations (100ppm, 150ppm, 200ppm) were investigated electrochemically after 288h immersion at 80°C and compared the results with that of testing without thiosulfate in the environment. According to the Potentiodynamic polarization test results, it is found that the presence of thiosulfate ($S_2O_3^{2-}$) in the solution hinders the passivation that was formed during the immersion of Zn alloys between 120h and 288h at 80°C in the absence of thiosulfate. Thiosulfate effect promotes Cl^- penetration for not only hinderance of the passivation but also generating the depassivation of passive films resulting in retarding repassivation. It is confirmed by the comparison between polarization test results of testing without thiosulfate and with thiosulfate in the solution. However, although all thiosulfate concentrations used in the study impedes the passivation, the different thiosulfate concentration gives the different effectiveness depending on the immersion time and temperature. Also, Al presence in the Zn alloys supports the different effectiveness. The lower thiosulfate concentration (100ppm) exhibits the decrease of current density at longer immersion for Z32120 whilst Z13000 exhibits the decrease of the current density at higher thiosulfate concentration (200ppm). Regarding the results investigated in this study, Z32120 is effective with 150ppm and 200ppm thiosulfate meanwhile Z13000 is better result with 100ppm and 150ppm. Therefore, 150ppm is considered to be the proper and average value for both Zn alloys. The effect of thiosulfate on passivation of both Zn alloys was discussed based on immersion time, temperature, pH, and the ratio of Cl^- and $S_2O_3^{2-}$.

Field of Study:	Metallurgical and Materials Engineering	Student's Signature .....
Academic Year:	2022	Advisor's Signature .....

ACKNOWLEDGEMENTS

First of all, I would like to express sincerely of my gratitude towards my advisor, Prof. Dr. Gobboon Lothongkum Ing., for his constant support of my thesis, resourceful knowledges, wise advice, patience, motivation and enthusiasm. His remarkable guidance always helped me with my research and writing of this thesis. Having the best advisor and mentor for my master's degree study is the unforgettable privilege during my educational period.

I am respectfully grateful to Dr. Pinai Mungsantisukmm, CEO of The Thai Marine Protection Co., Ltd, Thailand, for kindly providing the high quality of zinc alloys samples (Z32120 and Z13000). Also, I would like to thank to Mr. Tanapat Kaewmaneekul who worked hard on the research of creating these two zinc alloys (Z32120 and Z13000) and gave me the opportunity to do further research for my study based on his work,

I additionally would like to appreciate on all the professors, lecturers, and students in my department for helping me as possible as they could, along with Ms. Niramon Loplar (Department Officer). I am grateful towards my seniors, Mr. Songkran Vonsilathai and others for instructing and demonstrating the use of Potentiostat for electrochemical tests. Further, I would like to praise my fellow master student in the department and my friend, Mr. Pattarapong Wannapraphai, for his continuous helps in both educational life and personal life throughout all these years whenever I need to solve my language barriers in many aspects of daily life.

I want to acknowledge Ms. Chiraporn Tongyam (Chulalongkorn University), the technician who conducted FE-SEM on my samples with precise skills, patience and kindness.

Furthermore, apart form my advisor, I would like to show my humble gratitude to my thesis committes: Asst. Prof. Panyawat Wangyao, Ph.D, Dr. Nithi Senarjha, Ph.D, Dr. Wanida Pongsaksawad, Ph.D (Senior Researcher at Smart Manufacturing and Maintenance Technology Research Team, Rail and Modern Transports Research Center, National Science and Technology Development Agency), for their encouragement, insightful comments, helpful advices and hard questions.

Lastly, I would like to express my greatest appreciation for the financial support of ASEAN and Non-ASEAN Scholarship award by Chulalongkorn University and the Covid-aid financial support by Department of Metallurgy, Faculty of Engineering, Chulalongkorn University. Additionally, I would like to thank those whose names are not mentioned here, however, I have greatly been inspired and encouraged by those till the end of this independent study.

Thwelt Thinzar Zaw

TABLE OF CONTENTS

Page

LIST OF TABLES

Page

LIST OF FIGURES

Page

CHAPTER (1)
INTRODUCTION

1.1 Background

Cathodic Protection (CP) is one of the prevention methods for corrosion. There are two types of CP: Impressed Current and Sacrificial Anode. Sacrificial anode is consumed to protect the cathode which is the structure to be protected. Zn is one of the major anodes that are used in many operations. Sometimes throughout the operation at a platform (vessel), the solution temperature is possibly up to ~80°C from hours to days. At those kinds of conditions, Zn anodes are passivated, thus leading to the change in potential difference and polarity. Then, the structure becomes an anode leading to corroding. That is why they should not be used at temperatures higher than 50-60°C and due to the mechanical fragmentation by intergranular decohesion. However, although pure Zn encounters passivation, intergranular decohesion is not found. Based on the environments, the Zn corrosion product on the anode surface causes its own passivation. Thick crumbly porous white rust occurs in seawater. Either each existence of sulfate and chloride separately or both together can accelerate the formation of white rust leading to the formation of zinc sulfate, zinc hydroxysulfate and zinc hydroxychlorosulfate. Zn anodes are upgraded with alloying to avoid passivation increasing capacity and improving dissolution morphology and mechanical properties[1]. However, rather than developing new grades of Zn anodes by alloy additions, a better solution is to make a change of the environmental solution in the vessel which seems to be easier to inhibit the Zn passivation. Therefore, to have a better understanding of the inhibition on Zn passivation, it should be considered about addition of thiosulfate which is effective to inhibit or spall off the passive films in chloride solution.

There are two different sulfur functions of thiosulfate; an $-SO_3^-$ group in which sulfur has a nominal oxidation state of plus six, and an adjoining sulfide group of sulfur which has a minus two oxidation states. Thiosulfate salts are extremely stable and excellent complexing agents for metal ions, however, the sodium salt $Na_2S_2O_3.5H_2O$ is very soluble. The thiosulfate oxidation often leads to sulfate; the intermediate sulfite is not stable in the presence of oxidation products such as tetrathionates due to the chain

degradation reaction. Thiosulfate used in the bleaching industry as ‘antichlorine’ to remove excess chlorine losing eight electrons of the sulfide atom[2].

$$5H_2O + S_2O_3^{2-} + 4Cl_2 \rightarrow 2HSO_4^- + 8HCl \quad (1)$$

In the absence of oxygen, the corrosion process leads to the mackinawite scales formation meanwhile iron sulfide forms by the reduction of thiosulphate and sulfite. Sulfites subsequently give rise to sulphates and thiosulfate by further reaction with oxygen and sulfur. The role of thiosulfates in corrosion and its effects has been well known since the 1940s. In geothermal plants, the extracted fluid in a variety of concentrations depending on reservoir, contains non-condensable gases (NCGs) which contain mainly carbon dioxide, significant trace amounts of hydrogen sulfide[3]. The oxygen exchange between thiosulfate and water was measured in 1971 by Betts, proposing that sulfite appears as an intermediate species as at an intermediate pH. In 1975, Seibert showed that the sulfur atoms of thiosulfate can exchange positions in a thiocyanate melt at a high rate. Thiosulfates are technically prepared by oxidation of polysulfides in air and that was proved by Teder, 1965 and Gmelin, 1963[2].

General corrosion induced by Cl^- can accelerate by increasing $S_2O_3^{2-}$. Polythionates, especially thiosulfate ions ($S_2O_3^{2-}$) are one of the most harmful substances in oil and gas industries. In the presence of $S_2O_3^{2-}$, the typical types of corrosion are pitting, crevice corrosion, fatigue corrosion and stress corrosion cracking. To avoid potential hazards, $S_2O_3^{2-}$ is a safe substitute of H_2S for corrosion. $S_2O_3^{2-}$ can generate (via chemical or electrochemical reactions) elemental sulfur which has the ability to further change into H_2S by disproportionation or reduction. However, $S_2O_3^{2-}$ alone has not proved yet that it is deleterious enough to have the tendency to act together with other localized corrosion assisting ions to initiate the susceptible effect on metal. [4].

By the facts of thiosulfates that can be effective to the passive films formed by passivation in the presence of Cl^-, the research will be focused on its effect of inhibition before the formation of passivation. Further, if there is passivation, the research can clarify the effect of thiosulfate spalling off the passive films to give depassivation and prevents the repassivation on the anode surface.

1.2 Objectives

To study the effect of thiosulfate in 3.5%NaCl solution on the inhibition of zinc-alloyed anodes passivation at 80°C after immersion for 288h.

1.3 Scopes of research

The experiment is to

1. investigate if there would occur the passivation after immersion for 288h in the presence of thiosulfate.
2. clarify the inhibition of passivation on Zn alloyed anodes by the effect of thiosulfate.
3. study that thiosulfate can spall off the passive films on the anodes giving the depassivation mechanism.
4. research that thiosulfate can process the prevention from the repassivation after depassivation.

1.4 Advantages of the research

1. Clarification of the effect of thiosulfate on the passivation and depassivation of Zn-alloys in 3.5% NaCl solution.
2. The research will reveal the interaction between the thiosulfate and chloride penetration that causes the inhibition of passivation and the occurrence of depassivation of the sacrificial anode.
3. The research will investigate the pH change by chloride penetration at elevated temperature and its effect related to thiosulfate on passivation and depassivation.
4. The research can offer an approachable solution for the inhibition of the passivation and the solution for the depassivation of Zn sacrificial anode at 80°C by changing the solution environment artificially with thiosulfate.

CHAPTER (2)
LITERATURE REVIEW

2.1 Cathodic Protection

Cathodic Protection (CP) is one of the corrosion prevention methods which is widely used. It can principally reduce or prevent the corrosion of any metal or alloy that is exposed to any aqueous electrolyte. Moreover, this method can give the corrosion rate to virtually zero, and its proper system maintenance can also provide the corrosion protection indefinitely [5]. Last several decades indicated that cathodic protection is the most promising method for protecting in pipelines [6]. In the 1820s, the British pioneered in using the cathodic protection on copper fittings of wooden sailing vessels [5]. Sir Humphrey Davy XI reported this discovery in 1824 that copper could be successfully protected against corrosion by coupling it to iron or zinc. In the 1920s, cathodic protection was used for the first time to protect buried pipelines which were transporting and carrying petroleum products such as oil and gases, in the Gulf Coast oil fields of the United States. There became enormous developments of cathodic protection in the consecutive decades, such as in the 1950s; cathodic protection of steel-hulled ships became technically prevalent to the supplement of corrosion-resistant and fouling-resistant coatings. From the start of this century, thousands of miles of buried pipelines and cables have been effectively protected by cathodic protection. The common applications using cathodic protection are such as ships, offshore floaters, offshore drilling structures, subsea equipment, harbors, pipelines, storage tanks, concrete structures; all submerged or buried metal structures [5, 7].

Based on the type of the polarization used to protect the structure, cathodic protection systems are divided into impressed current systems or sacrificial anode [7]. As the fundamentals, cathodic protection reduces the corrosion rate by cathodic polarization of a corroding metal surface as the cathode with the use of an impressed current (Fig 2-1) or attachment of a sacrificial anode. This is an electrochemical method that uses cathodic polarization to control the kinetics of the electrode process occurring on the metal/electrolyte interface. The respective anode (Eq.2) and cathode (Eq.3) reactions [5, 7] for iron corroding in an aerated neutral electrolyte are:

$$Fe \rightarrow \quad Fe^{2+} \; + \; 2e^{-} \tag{2}$$

$$O_2 + 2H_2O + 4e^{-} \rightarrow 4OH^{-} \tag{3}$$

These two half-cell reactions are combined to form the overall corrosion reaction[8]:

$$2Fe + O_2 + \; 4e^{-} \rightarrow Fe(OH)_2 \tag{4}$$

Impressed current system requires the external DC current, which is supplied from a power source such as rectifier, using as a cathodic polarization on the structure to be protected with the result of high current capacity. Therefore, impressed current system can be used to protect even the bare and poorly coated pipelines. However, all impressed current systems require the routine maintenances compared to sacrificial anode systems because of the existence of power supply and more electrical connections[7, 9]. The corresponding applied potential and current density are necessary to be varied accordingly and so are several tedious automated controls in necessity, therefore, controlled potential systems are used in these conditions. This kind of cathodic protection is widely used for ship hulls and several seawater installations where the flowing water velocity is variable [7]. Since impressed systems contains a rectifier converting the alternating-current to direct-current, replaces the sacrificial anode, a source of alternating current must be close to the structure. However, the range between the alternating current and the structure may be a problem in areas that are remote or difficult to process. Therefore, sacrificial anodes should be inserted as the source of current in these cases [8]. In aerated neutral or alkaline solutions, cathodic corrosion reaction is usually the oxygen reduction and controlled by the oxygen availability for diffusion to the cathodic corrosion site. However, for the immersed structures in flowing water, the water flow velocity will change the variety for limiting current of oxygen. Then, that will lead to either under-protection or over-protection [7].

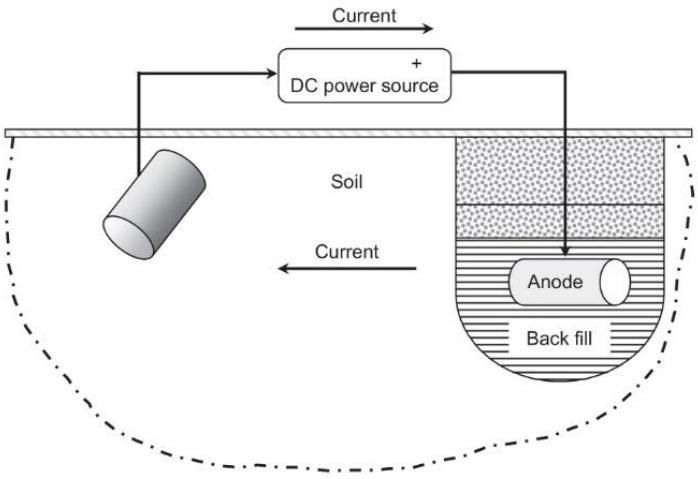

Figure 2-1. Schematic of the impressed current system cathodic protection [7]

In the system of sacrificial anode, the protection is facilitated by coupling a less noble metal with the structure (Figure 2-2). Less noble means more electronegative in the galvanic series. The polarization is accompanied by a flow of ionic current through the solution from the more negative metal (anode) to the more positive metal (cathode) which means that when a less noble metal is electrically coupled to a more noble metal, it will corrode itself anodically dissolved to protect (cathodically polarized) the more noble metal which acts as a good cathode for the cathodic reaction [6, 8, 10]. This is a phenomenon that the anode acts as 'sacrificial anode' consuming more rapidly than the structure (cathode) in the supplement of electrons. Sacrificial anodes do not require the outside power sources but serve as a source of electrical energy and they rather provide their own power with the need of minimum maintenance[6, 7, 9]. This kind of system possesses an open-circuit potential with more negative potential difference than the structure to overcome the formation of anode-cathode cells. When the current is generated, the anode should not be polarized significantly. The anode must have high anode efficiency that is the current produced by the metal dissolution must be readily available for the cathodic protection. The extent of anode life protecting the structure, depends on its attained potential which relies on electrochemical properties governed by such as compositions and the exposed environments [10]. Usually, high purity anodes such as zinc, aluminium, magnesium, are used to avoid significant anode polarization and accumulation of insulating reaction products. Sacrificial anodes are

well-coated structures with minimum chance of damage during service life. The backfill which is used to contain the anode is usually made of suitable material; gypsum (72%)/bentonite (20%)/sodium sulfate (5%) to maintain the current flow and absorb corrosion products and water from the soil to keep the anode active.

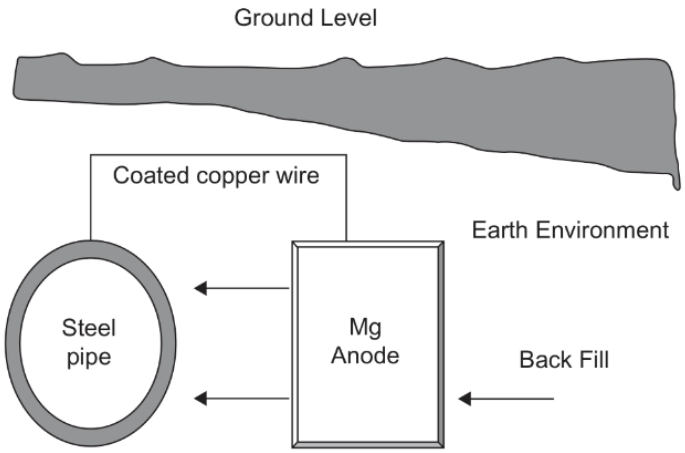

Figure 2-2. Schematic of sacrificial anode system cathodic protection [7, 9]

2.2 Sacrificial anodes

Since the sacrificial anodes must be more electronegative than the structure[7], thus, there is a limitation in range on the availability of suitable materials to protect the specific structure. This range is restricted by the rapid and extreme corrosion of most negative potential metals in aqueous environments. Hence, alloys of only magnesium, aluminium and zinc are possible for utilities [10].

2.2.1 Basic Composition

The other constituent elements except the basis metal, happen to be exited as impurities either in the raw materials or intentional alloying additions. To counter the bad anode working by impurity elements, the necessity is the control of input materials quality so that the required anode ability is to be achieved [10].

There are basis three generic metal types shown in Table 2-1 for sacrificial anodes; zinc, aluminium, magnesium which are used to avoid significant anode polarization and

accumulation of insulating reaction products [6]. Magnesium alloys which are more frequently used, have very negative operating potentials and possess to provide a large driving voltage for cathodic protection [8]. Zinc and aluminium alloys are more modest compared to magnesium alloys. On the contrary, aluminium alloys provide enough current capacity to be doubled in comparison of zinc and magnesium alloys. In practice, selection is significantly more complicated and detailed.

Table 2-1. Typical basic material composition requirements for anode[10]

99.90% Magnesium	99.99%Zinc	99.95% Al(P0610)	99.90% Al(P0506)
Cu 0.02 max	Pb 0.003 max	Fe 0.10 max	Fe 0.06 max
Mn 0.01 max	Cu 0.001 max	Si 0.06 max	Cu 0.003 max
Sn 0.01 max	Cd 0.003 max	Cu 0.003 max	Ni 0.003 max
Ni 0.001 max	Fe 0.002 max	Ni 0.003 max	Si 0.05 max
Pb 0.01 max	Sn 0.001 max	Cd 0.002 max	Cd 0.002 max
Others 0.05 max	Zn 99.99 min		
Mg 99.90 min			

2.2.2 Impurities

The dissolving metal should release all electrons to the structure supporting the cathodic reaction rather than waste them in local cathodic reactions on its own surface. In all standard sacrificial anode alloys, the presence of Fe is susceptible due to an intermetallic compound formation which acts as a good cathode between Fe and the basis metal. The existence of such cathode material will often raise the anode in operating potential (making it less negative) and promote within the actual passivation, therefore, the driving force from the anode is deducted or perished.

There are two ways of avoiding the problem Fe existence: control the Fe addition into the base metal or to drive Fe away to be ineffective. In fact, it is impossible to permit above Fe content limitation because moving away is only way to be more economic and practical within the defined limits. In contrast, other heavy metal impurities such as Cu and Ni, have the same adverse effects on all standard alloy types. One important condition is that these impurities are the deliberate choice at some point

as a supplier since it can be a delirious impurity to one application but may be a beneficial ingredient to another.

2.2.3 Alloying Additions

The adverse effect of impurities can be controlled by alloying additions, for instance, Si and Al are added to Zn and Mn to Mg, in order to counter the Fe effect [10]. In the CO_2/H_2S environment, decohesion occurs due to the hydrogen embrittlement failure[11]. To overcome this failure, a small amount of Ti is added. However, despite meeting the requirements of chemical composition, other factors such as metallographic structure, hardness, etc., still cause the anode to encounter the failure [12]. Moreover, alloy additions have other purposes to improve the anode performance by reducing the anode potential on operation that increase the driving voltage in order to avoid passivation, to increase the anode capacity, to develop the dissolution morphology, to adjust the mechanical properties of the dissolution product for detachment and to upgrade the anode mechanical properties. The Standard alloys are shown in Table 2-2 for Al alloys, Table 2-3 for Mg alloys and Table 2-4 for Zn alloys [10].

Table 2-2. Standard Al alloys[10]

Alloy Component (wt%)	Al-Zn-Sn	Al-Zn-Hg	Al-Zn-In
Fe	0.13 max	0.08 max	0.12 max

Zn	4.0-6.0	0.35-0.5	2.0-6.5
Si	_	0.11-0.21	0.05-0.020
In	_	_	0.01-0.02
Hg	_	0.0.35-0.050	_
Sn	0.1	_	_
Cu	0.01 max	0.006 max	0.006 max
Ti	0.02 max	0.02 max	0.02 max
Others	0.02 max	0.02 max	0.02 max
o/c potential vs. Ag/AgCl/seawater	-1.10V	-1.05V	-1.10V
Capacity (A.h/kg)	Variable	2830	2700

Table 2-3. Standard Mg alloys[10]

Alloy Component (wt%)	Mg-Mn (Galvomag^{R})	Mg-Al-Zn (high purity)
Cu	0.02 max	0.02 max
Al	0.01 max	5.3-6.7
Si	_	0.10 max
Fe	0.03 max	0.003 max
Mn	0.5-1.3	0.15 min
Ni	0.001 max	0.002 max
Zn	_	2.5-3.5
Sn	0.01 max	_
Pb	0.01 max	_
o/c potential vs. Ag/AgCl/seawater	-1.7	-1.5
Capacity (A.h /kg)	1230	1230

Table 2-4. Standard Zn alloys[10]

Alloy Component (wt%)	ASTM B4 18-88 Type 1	ASTM B4 18-88 Type 2	US Mil Spec A 18001K	DNV Elevated temperatures
Al	0.10-0.50	0.005 max	0.10-o.50	0.10-0.20
Cd	0.025-0.07	0.003 max	0.025-0.07	0.03-0.06
Fe	0.005 max	0.0014 max	0.005 max	0.002 max
Cu	0.005 max	0.002 max	0.005 max	0.005 max
Pb	0.006 max	0.003 max	0.006 max	0.006 max
Si	_	_	_	0.125 max
Others(total)	0.1 max	0.1 max	0.10 max	_
Zn	Remainder	Remainder	Remainder	Remainder
o/c potential Ag/AgCl/seawater	-1.05V	-1.05V	-1.05V	-1.05V
Capacitor (A h kg^{-1})	780	780	780	780

2.2.4 Production Factors

The production method of the sacrificial anodes must not compromise the benefits of alloy formulation. A variety of undesirable anomalies during production give negative effects from the desired anode properties during the service life. Some of these are discussed below.

The method of gravity casting affects the anode structure physically by the influences of associated cooling process on the segregation or distribution of alloying constituents, thus, segregation is unwanted in some case, due to the possibility of preferential attack on grain boundaries.

Significant porosity inside the anode indicates both the dissolved gases existing in the molten alloy and poor foundry practice. Also, porosity can be a cause for rejection and further investigation. [10]. Nonmetallic inclusions such as silicate inclusions and spherical oxide inclusions can cause anode failure. Moreover, silicate inclusions can destroy the continuity of the matrix becoming a source to crack under the action of stress. Along with the nonmetallic inclusions, heterogeneity and mechanical properties

are the internal causes for the failure of anode due to the impact energy indicating the poor toughness. Inclusions are same as dislocations and grain boundaries and known to be crystal defects due to the microstructure, thermal treatment process and other factors. The corresponding strain field at these crystal defects interacts with the strain field of hydrogen atoms, which are trapped in small mass by the defects, increasing the trapping time of hydrogen atoms to cause the diffusion and transport of them in the material. In the CO_2/H_2S environment, when the trapped hydrogens accumulate and combine to form molecules, they expand rapidly in volume producing the large hydrogen pressure which can increase to the level of atomic bonding forces to breakdown the local atomic bond leading to generate small microcracks [12].

Formation of cracks in the anodes (some cases) meanwhile of casting conducting, is inevitable due to the stresses affected by cooling which occurs particularly between the expanding of mold (heating) and the contracting anode (cooling) [10]. Hydrogen atoms adsorbed can diffuse through the cracks on the surface into the anode metal. The tensile stress which is the external cause to the anode failure, promotes the hydrogen diffusion and permeation, as well as cathodic reaction, to increase the hydrogen content inside the anode for trapping at the defects and it also increases the anode sensitivity to subcritical cracks. Under the action of tensile stress and hydrogen, hydrogen embrittlement fracture failure of the anode can be happened due to the decrease of cathode yield strength [12].

The anode material must be firmly attached to the cathode (structure) to necessarily induce the current from the anode remaining effective on the cathode, within its design life. As a consequence, the casting must essentially have the surface preparation of the structure insert to make sure a strong bond with the anode material. However, voids at the interface of anode can cause the bond integrity, so they are undesirable. Dry blast cleaning near white metal druing casting is the normal preparation for aluminum alloy anodes, and coating by hot dip galvanizing or electro-galvanizing is used for Zn or Mg anodes. Zinc coating with inserts for Al anodes must not be used as it leads the molten alloy to dissolve the insert [10].

2.2.5 Environmental Factors

The conditions of environmental exposure play a key role in determining anode performance. Specific environments often permit the use of particular anode materials[10]. In a complex acidic corrosive medium such as the coexistence of CO_2 and H_2S, the cathodic reactions undergo hydrogen evolution to generate hydrogen and hydrogen atoms diffused into the anode, later accumulating the crystal defects, thereby inducing hydrogen-induce microcracks, at last hydrogen embrittlement failure for the anode. However, a wet CO_2/H_2S environment gives the better protection effect of the anode in the exception of needing good hydrogen resistance for the preparation of the cathode of the sacrificial anode [12]. Environmental resistivity and chloride content will affect the anode performance. The chloride existence inhibits the passivation of Al alloy anodes; however, land-based applications generally cannot give sufficient chloride levels for this purpose. The capacity of an anode is dependent on the anode operating current density which will be governed by its environment for some extent matters, but partly within the control of the design. The proper anode size will give the avoidance certainly to the fully suitable current densities. Prolonged periods of low operating current density can lead to passivation resulting in the failure to activate when the required current for operation increases.

The importance of the temperature of the anode performance is essential especially when they are buried. For the pipelines which are being protected often by the sacrificial anode and containing the hot-products, temperature effects must be considered. At elevated temperatures, passivation of both aluminium alloys and pure zinc can occur. Zinc anodes have experienced problems at nearly 70°C in saline mud, suffering intergranular decohesion, however, the initiation for the damage has occurred to be nearly at 50°C and not recommended to use above 40°C although special zinc-based materials for temperature exceeding 50°C have been developed. However, pure zinc free of intergranular decohesion will passivate under the same conditions. The cathode material for the sacrificial anode is recommended to have both good hydrogen resistance and the extension of exposure time at high temperatures [12]. Most anode testing and development for utility at elevated temperatures are observed both in laboratories and in the field under isothermal conditions. There are some lab tests

carried out for Al and Zn anodes salinity (Figure 2-3) and Al in seawater (Figure 2-5) between 15- 20°C with the same interval of time. (Figure 2-4) provides the lab test of Al and Zn in chloride ion concentration [10].

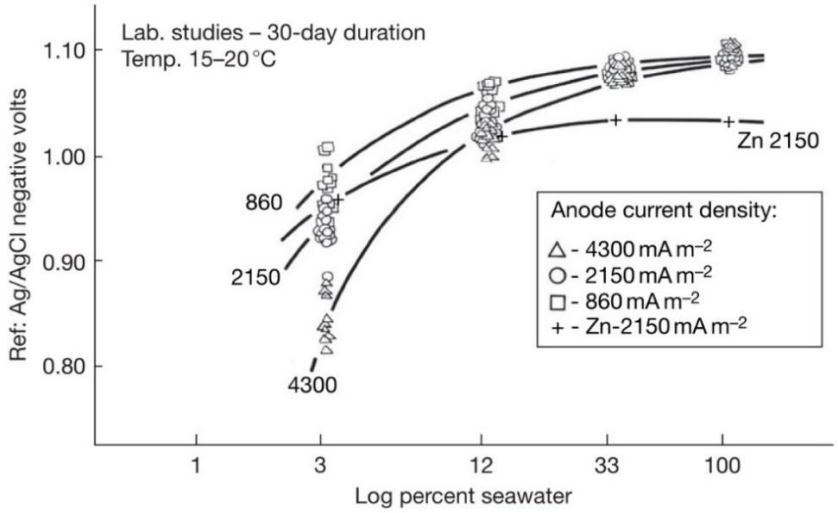

Figure 2-3. Electrochemical potential of Al and Zn anodes as a function of salinity and current density[10]

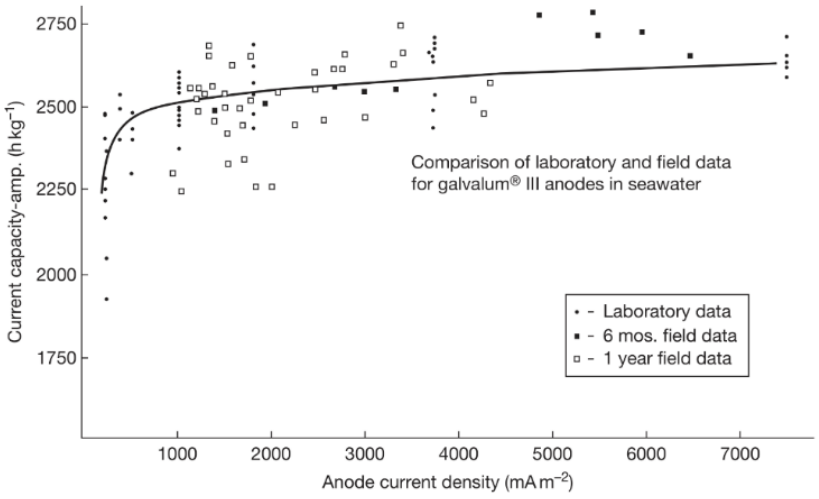

Figure 2-4. Capacity of Al and Zn anodes as a function of chloride ion concentration and current density [10]

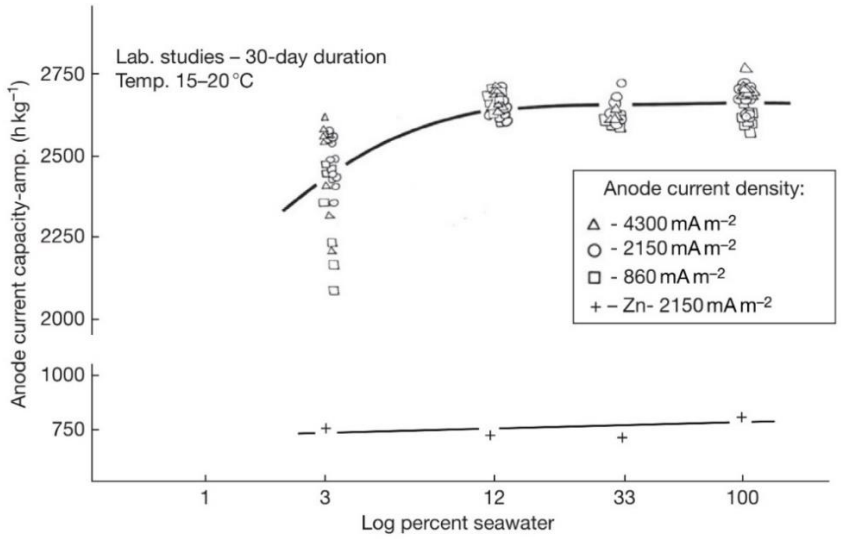

Figure 2-5. Capacity of an Al anode as a function of current density in seawater [10]

2.3 Applications of Sacrificial Anodes

The very first work on the sacrificial anode application was recorded in the 1820s by Sir Humphrey Davy. The work was focused on how to reduce the corrosion of copper sheets attached to the wooden hulls of naval vessels. Later, it was demonstrated with the sacrificial anode process expanding in large scales, then, finally in full-scale trials on the HMS Sammarang and the Carnbrea Castle using cast iron anodes.

Later in the 19th century of iron hulls popularity, zinc sacrificial anodes were used to protect against corrosion; however, the adherent nonconducting corrosion products resulted on the anode by impurities, particularly iron. Those suppressed the protection current flow which led to reduce the driving potential to the undesirable level [10]. The applications of sacrificial anodes involve with examples; ship, hulls and ballast tanks, offshore oil and gas drilling rigs, production platforms semisubmersibles and support facilities, water tank interiors, well castings, underwater pipelines, underground pipelines, buried structures, harbor piling and jetties, piers, floating dolphins, buoys, lock gates, and submerged concrete structures, desalination plants. There are many other uses including a large range of industrial equipment, for instance, heat exchangers, pump impellers and vessel internals [10, 13].

2.4 Selection of proper anode

2.4.1 Zinc

Zinc is the most reliable with few exceptions such as using in high temperature operation, compared to all anode materials and it has reliable electrochemical performance, ideal combination of intermediate corrosion potential, low polarization, and high efficiency in seawater applications. Due to the lowest driving voltage of the generic alloy types, therefore, it is unsuitable in highly resistive soils (except possibly as a ribbon), and in low salinity waters. If an operational potential is low and insufficient, the privilege (overprotection) concerns coating disbondment and hydrogen damage of the high strength steel. Zinc anodes have a poor capacity compared to aluminium. However, passivation is hard to occur on zinc in low chloride environments or with a consequent periods of low operating current density. The reliable operational characteristics of zinc often surpass aluminium with costs about half the price in the point of economic attraction since aluminium can passivate under such conditions. However, zinc anodes are not suitable to use in applications at temperature more than 50°C and not predominant in onshore or offshore application, but they find use under both conditions [5, 10].

2.4.2 Aluminium

Aluminium alloys are developed to use as sacrificial anodes in sweater in the presence of chloride due to very high output since aluminium contains high valence and low density[5]. The great attraction of aluminium anodes is their less constancy in electrochemical characteristics and extremely high capacity over three times that of zinc and the cost of view along with the substantial weight savings which can be of great importance. Aluminium anodes are composed essentially of three generic types: Al-Zn-In, Al-Zn-Hg and Al-Zn-Sn. Indium and mercury are added to aluminium to function as activators to overcome the natural passivation of aluminium. Despite this fact, aluminium anodes are not suitable for low chloride environments which would lead to passivation. Aluminium alloys are susceptible to thermite sparkling when dropped on to rusty surfaces. Therefore, their use should be restricted since thermite

sparking has the effect on the kinetic energy of the anode released on impact which can be failed [10].

2.4.3 Magnesium

Magnesium has highly active corrosion potential and low polarization to use primarily in soils or pure water where electrolyte resistance is high. Also, it is nontoxic to use even in potable water systems wherein the conductivity is low. It has high driving voltage resulting in overprotection which is an advantage for the spalling off the coating bond. However, magnesium is usually not used for seawater applications due to its overprotection, inefficiency, and consequent low anode life. For some exceptions with alloying to deactivate magnesium, it can be used in lower resistivity environment. There are two generic types of magnesium: Mg-Mn and Mg-Al-Zn. Both alloys system has a high driving voltage as a result to be able to use in the application in high resistivity environments: soils and fresh, or brackish waters. Relatively poor capacity along with the high unit cost are disadvantages that magnesium rarely finds application in subsea environments, however, alternatives are available. Magnesium is susceptible to thermite sparking when dropped on rusty surfaces, therefore, applications involving a spark hazard, for instance, tankers carrying inflammable petroleum products are unsuitable to us magnesium anodes [5, 10].

2.5 Anode system Life

The designed life of cathodic protection is as short as 1 year or more than 40 years. The longer the protection lifetime, the greater the mass or anode material is required. There are some factors for anode life system as follows [10]:

1. Calculating the weight of individual anode
2. Anode size and shape
3. Anode output
4. Anode resistance
5. Anode lifetime for protection
6. Number of anodes
7. Anode (End Current) distribution

8. The anode-insert
9. Utilization Factor
10. Backfills for anodes

2.6 Passivation on Zinc

The dissolution and precipitation of passive films on pure Zn and Zn-Al alloys can be affected by the temperature of 80°C and passivation happens, however, it does not appear at 25°C. This fact was proven by T. Kaewmaneekul et al.[1] to support the argument that pure Zn and Zn-Al alloys can be passivated at higher temperatures. The dissolution rate of Zn increases with increasing temperature. Hence, this implies that Zn^{2+} dissolves sufficiently to interact with anions in solution at 80°C by precipitating the passive film at surface according to the overall possible reactions (4-12) [1].

Occurrence of active dissolution of Zn species (for pure Zn in artificial seawater):

$$Zn \rightarrow Zn^{2+} + 2e^{-} \quad (5)$$

$Zn(OH)_2$ and ZnO films formation on Zn surface when passivation occurs:

$$Zn^{2+} + 2OH^{-} \rightarrow Zn(OH)_2 \quad (6)$$

$$Zn(OH)_2 \rightarrow ZnO + H_2O \quad (7)$$

When CO_2 dissolves from atmosphere into solution, HCO_3^- can be formed:

$$CO_{2(g)} \rightarrow CO_{2(aq)} \quad (8)$$

$$CO_{2(aq)} + H_2O \rightarrow HCO^{-}_{3(aq)} + H^{+}_{(aq)} \quad (9)$$

Interacting of HCO_3^- with Zn^{2+} and H_2O by hydrolysis reaction:

$$5Zn^{2+} + 6H_2O + 2HCO_3^{-} \leftrightarrow Zn_5(CO_3)_2(OH)_6 + 8H^{+} \quad (10)$$

Zn^{2+} and H_2O further reacts with Cl^- and SO_4^{2-} to form other compounds and H^+ corresponding to the possible hydrolysis reactions:

$$5Zn^{2+} + 9H_2O + 2Cl^{-} \leftrightarrow Zn_5(OH)_8Cl_2.H_2O + 8H^{+} \quad (11)$$

$$4Zn^{2+} + 10H_2O + SO_4^{2-} \leftrightarrow Zn_4SO_4(OH)_6.4H_2O + 6H^{+} \quad (12)$$

$$12Zn^{2+} + 20H_2O + 3Cl^- + 3SO_4^{2-} \leftrightarrow Zn_2(OH)_{15}(SO_4)_3Cl_3.5H_2O + 15H^+ \quad (13)$$

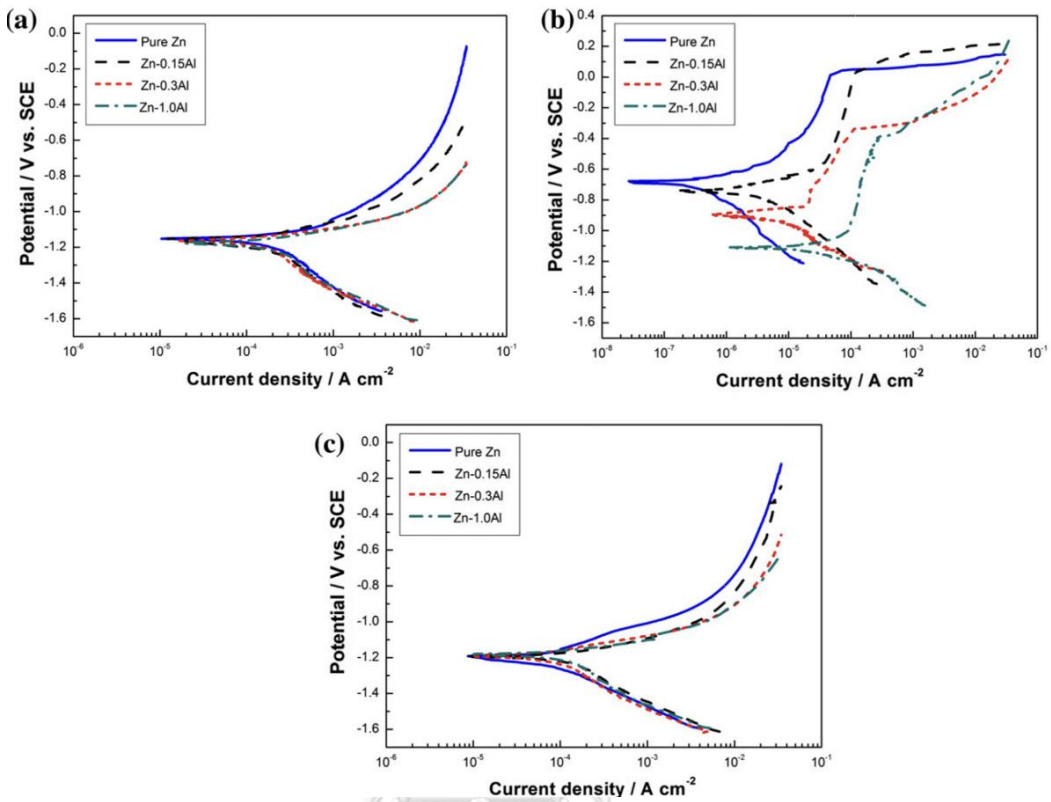

Figure 2-6. Potentiodynamic polarization curves of different Zn alloys at (a) 48 h, (b) 288 h and (c) 720h of immersion in artificial seawater at 80°C [1]

T. Kaewmaneekul et al. [1] proved that not only the high temperature but also the immersion time can affect the passivation on pure Zn and Zn-Al alloys. After immersion for 48 h, pure Zn and Zn-Al alloys exhibit no passivation, but different anodic current density which Zn-Al alloy is superior to pure Zn. At the immersion time of 288h, all metal samples have experience of passivation and the author claimed that the passivation is caused by the various protective compounds or corrosion products on the surface. In the passive region, average passive current density (i_{pass}) of Zn-Al alloy is higher than pure Zn with average value of ~20.4 μAcm^{-2}, however, that value is less than that of Zn-1.0Al alloy which is ~127 μAcm^{-2}. At last, when the samples in immersion for 720h were tested with the approximately similar current density which used for 48h in immersion, all pure Zn and Zn-Al alloys appeared to have no passivation which was suggested to be the films dissolution instead of no passivation. This

phenomenon is the mechanism between passivation and depassivation related to the immersion time shown in (Figure 2-6).

Passivation of Zn in alkaline solution is by means of the dissolution and precipitation mechanisms. And the physical and chemical properties of the corrosion product on Zn depend on temperature. The maximum metal corrosion rate in many environments occurs in the temperature range of 55-65°C. The the attack on Zn in the deaerated solution is considerably affected by the temperature rise.

V. Ashworth et al. [14] gave a reference on the fact that temperature is one of two interacting variables to control the onset of a potential reversal meanwhile another variable is solution composition. If Zn becomes more noble than steel, the conditions are so called “potential reversal”. In deaerated solutions, potential reversal is unable to occur, however, in aerated solutions, it might occur in the presence of bicarbonate or nitrate ions. The presence of chloride or sulfate ions decreases the possibility of potential reversal occurrence. In borderline cases, an increase in temperature can favor potential reversal. Ashworth used another reference that reversal did not occur in a deaerated solution up to 85°C. Ashworth also stated another reference that the passivation of Zn happens due to the potential reversal, and species in the solution will prevent both passivation and potential reversal. Usually, in the presence of chloride ions, the potential reversal does not occur since the corrosion potential of the steel is more noble than the critical breakdown potential of Zn. However, there are circumstances which existed to occur the potential reversal even in the presence of chloride ions by marked pitting of the Zn. In the presence of oxygen, Zn undergoes spontaneous passivation resulting the visible pits which increase in size leading to reduce the local cathodic current density and give rapid metal dissolution rate for constant corrosion products occurrence. Repassivation, therefore, is possible and the potential fluctuations in the breakdown potential region at 50 and 90°C due to pitting effect and pit sites by corrosion product on the surface.

The steady decay of galvanic current and the continuous rising in the electrode potentials in oxygen saturated solution at 90°C, can suggest that both the cease of steel cathodic protection and an impossible exclusion of potential reversal under any coupling experiments. At various temperatures of Ashworth’s examination (30, 50, 75

and 90°C, ±1°C) of Zn surface. The polarization curves between the deaerated solution and the oxygen saturated solution have a comparison which reveals that the corrosion potential of Zn always lies above or very close to the critical breakdown potential at each focused temperature, in the range of 30 to 90°C, in the latter case shown in (Figure 2-7) and (Figure 2-8).

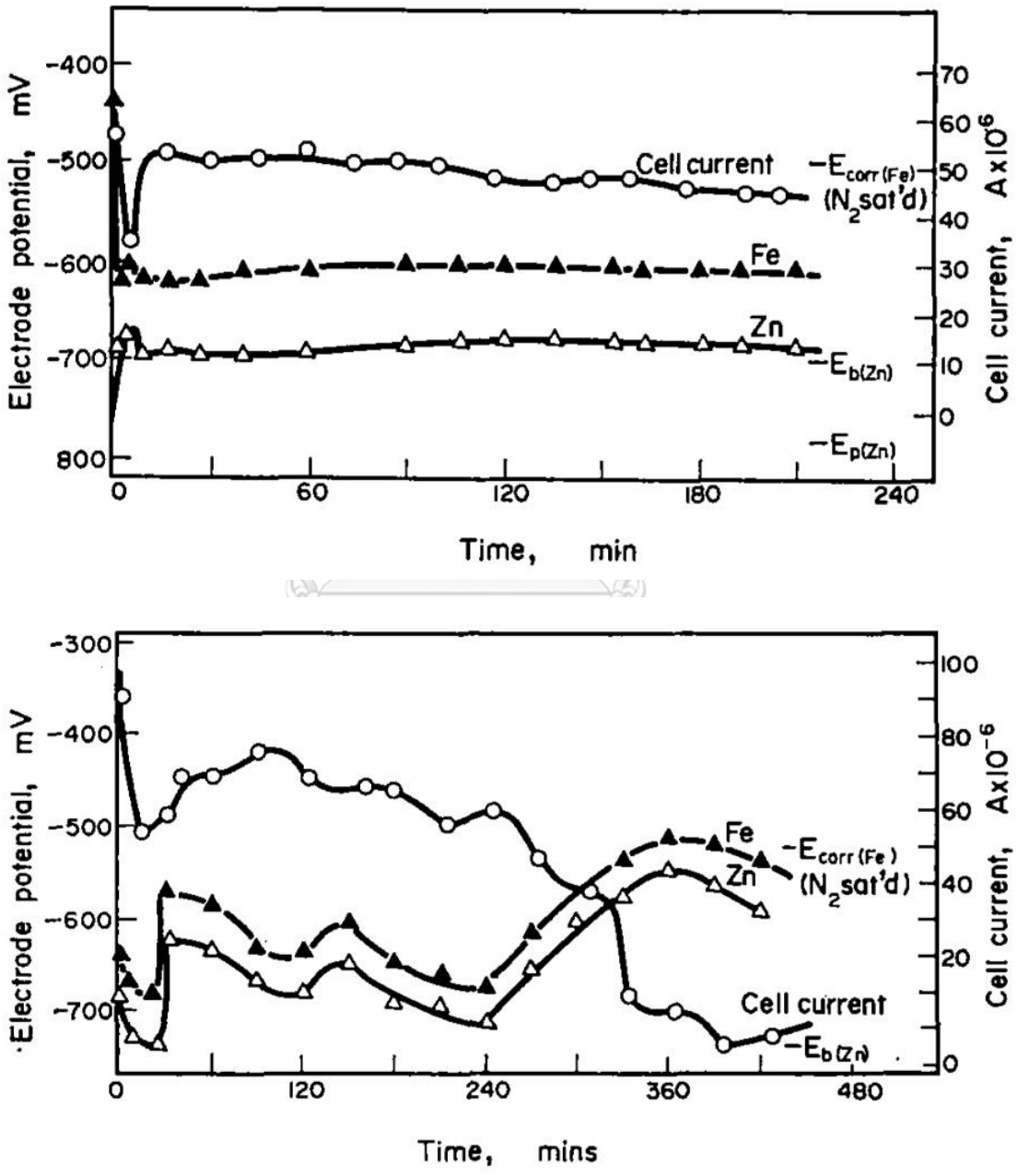

Figure 2-7. Zinc electrode potential as the galvanic coupling in the oxygen saturated solution at 30°C (above) and 90 °C (below) [14]

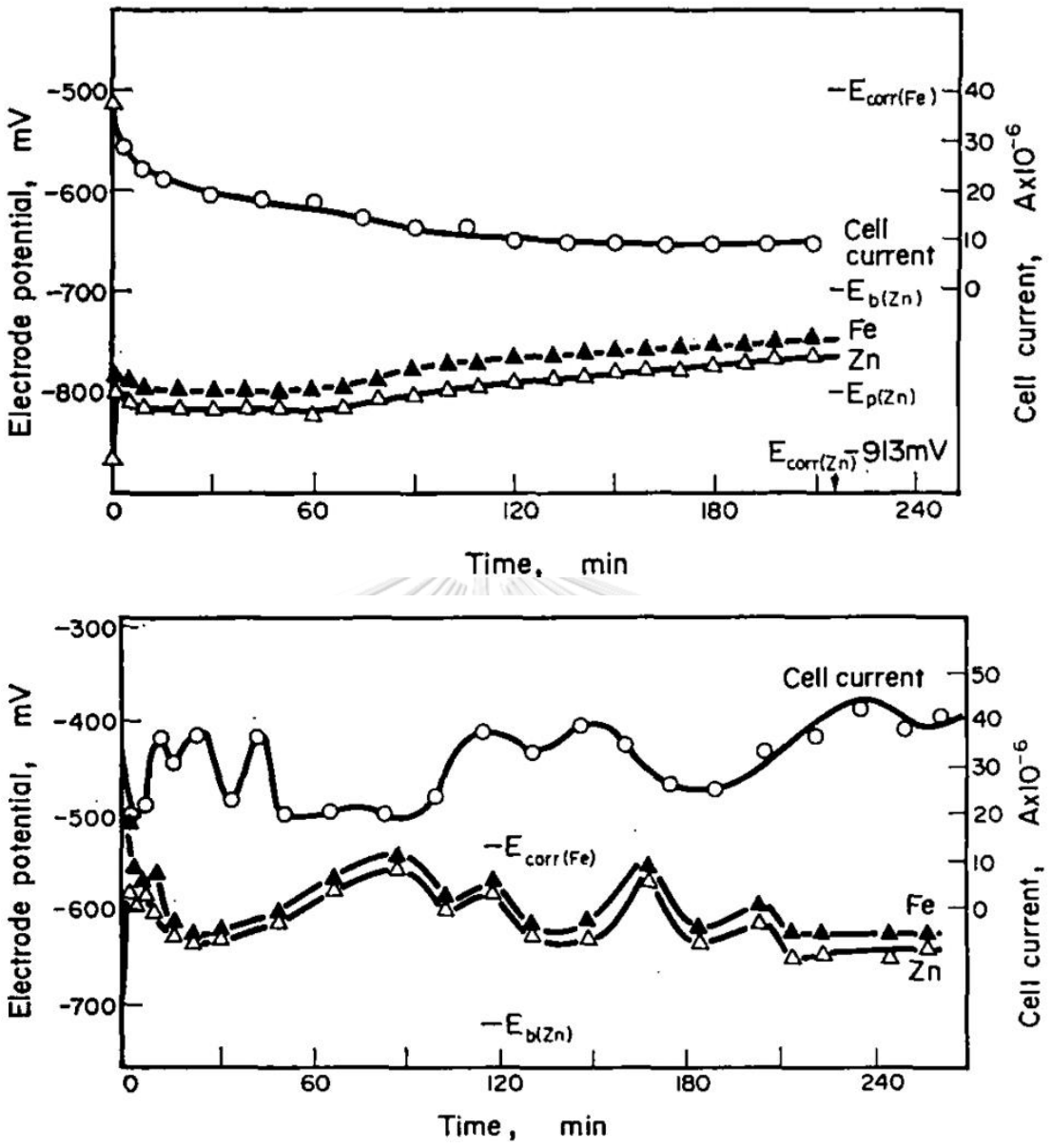

Figure 2-8. Zinc electrode potential as the galvanic coupling in the dearated solution at 30°C (above) and 90 °C (below) [14]

2.7 Thiosulfate

2.7.1 Effect of Thiosulfate on Oxygen

In the absence of thiosulfate, sulfite addition can cause a rapid depletion of dissolved oxygen and the reaction leads to a variation in pH shown in (Figure 2-10) by the acidity increasing with the amount of reacted sulfite. The variation in oxygen concentration between additions can become greater with increasing sulfite content. Lower amounts of sulfite are used in industrial plants for oxygen scavenging purposes, and they react with oxygen dissolved in the water, causing its removal. The thiosulfate presence affects the oxygen-scavenging reaction promoted by sulfites. Particularly, they are studied as inhibitors of the formation of sulfates in sulfur abatement implants form combustion gases by Ulrich et al. [15] and Mo et al. [16] The inhibiting effect depends on the sulfite/thiosulfate ratio shown in (Fig 2-11); the addition of increasing amounts of sulfite over thiosulfate hinders the effect of the thiosulfates and gradually increases the oxygen-scavenging rate. The action of thiosulfate increases not only the oxygen levels not only in sulfite containing solutions but also the corrosion rate due to its concentration. Furthermore, it increases the kinetics with a major effect on the cathodic reaction along with greater water flow and lower pH. The reduction of thiosulfate reduces the concentration of hydrogen ions which tend to increase pH on the metal surface, especially under conditions of high corrosion rate. Moreover, the oxidation of sulfite to sulfate causes a decrease in pH. The effect of pH on polarization curves can be seen in (Figure 2-12). In the experiments of M. Cabrini et al. [3] thiosulfate ions tend to block the oxygen-scavenging reaction, and thus, stabilizes the pH, slowing down the production of acidity. The time dependence of pH in aerated solution is also shown in (Figure 2-9). The author, M. Cabrini also stated in his work that Kappes [17, 18] pointed out the fact which the corrosion rate in solutions containing thiosulfate is higher than in the same solution devoid of it. However, it is saturated with an H_2S partial pressure which is equal on the surface in the presence of thiosulfate.

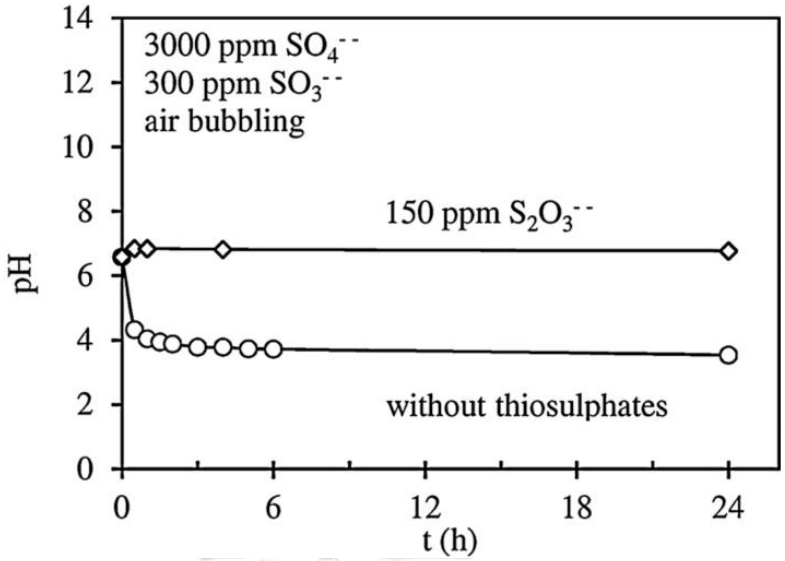

Figure 2-9. Time-dependence of the pH of aerated solutions[3]

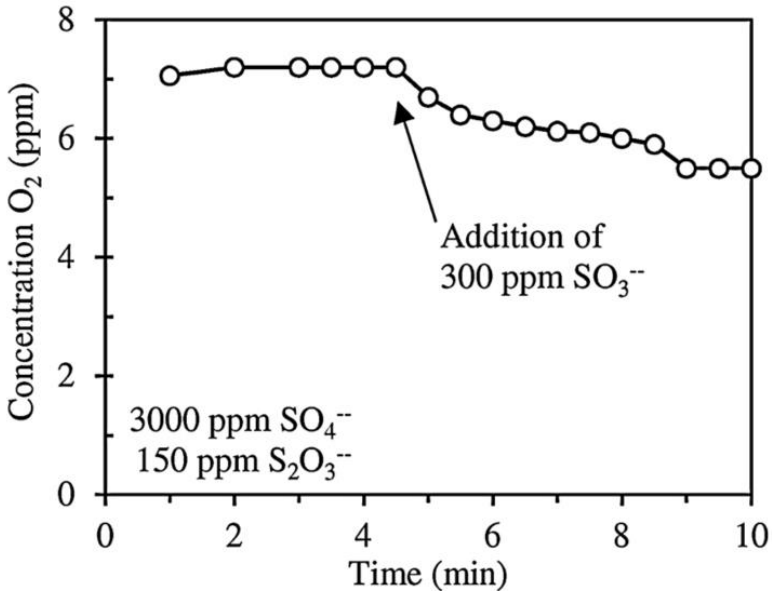

Figure 2-10. Variations in dissolved oxygen concentration following the addition of sulfite to a solution of sulfate containing thiosulfate [3]

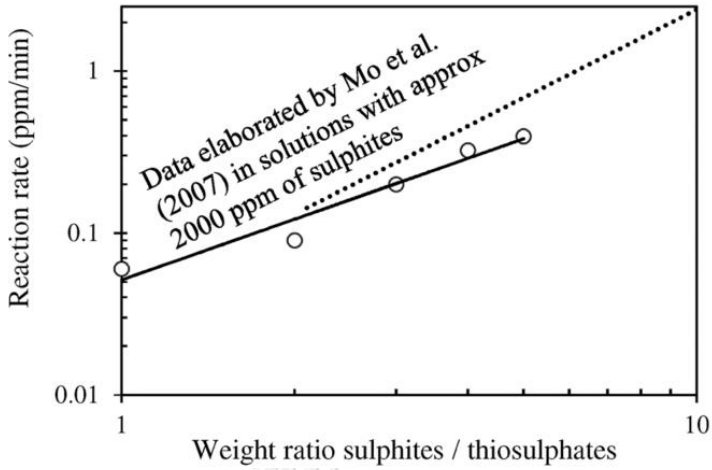

Figure 2-11. The dependence of oxygen reaction rate on the sulfite/thiosulphate ratio (decreases in dissolved oxygen content per time unit) [3]

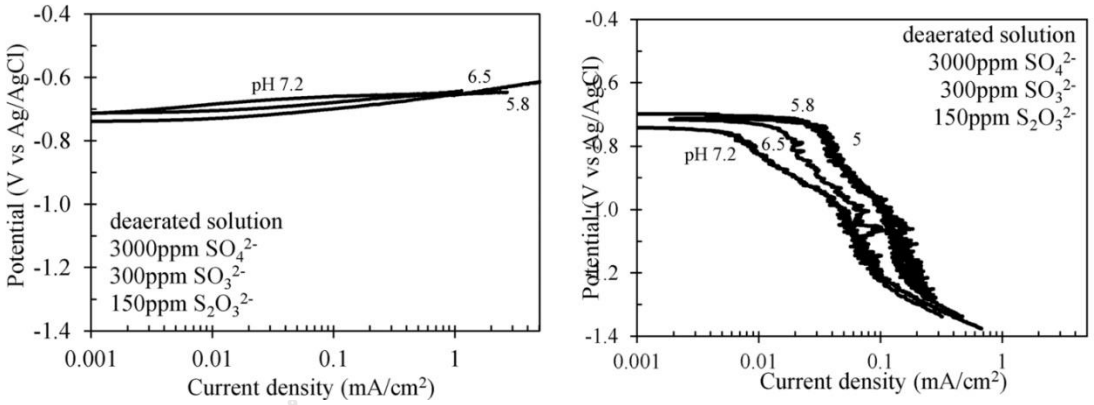

Figure 2-12. Effect of pH on the polarization curves conducted with stationary electrodes. Anodic curve (left) and cathodic curve (right) [3]

2.7.2 Effect of Thiosulfate on Chlorine

General corrosion is induced by Cl^- accelerated with the increase of $S_2O_3^{2-}$ concentration. The Cl^- ion initiates pitting sites on the metal by breaking down the passive film and $S_2O_3^{2-}$ impedes or inhibits the repassivation capacity of the passive film resulting in stable pit formation. The ratio of chloride ions and thiosulfate varies depending on the microstructure of the metal. If the activity of $S_2O_3^{2-}$ ions is higher compared to the Cl^- ions, the passive film would have improved effect. Inclusions and coarse-grain structure in the microstructure can improve the electromigration of Cl^- ions

into the passive film. At higher concentration, $S_2O_3^{2-}$ might be absorbed as elemental sulfur into the metastable pitting sites. The adsorbed elemental sulfur actively blocks the adsorption of OH^- ions into the passive film which ultimately slows down the repassivation process of the passive oxide film in Cl^- solution. Of all the sulfur species, thiosulfate ($S_2O_3^{2-}$) came from sulfate and elemental sulfur, is one of the most intriguing, metastable polysulfur oxyanions which can undergo both oxidation and reduction or disproportionation and decomposition. The nature of corrosion is determined by the concentration of $S_2O_3^{2-}$ ions in Cl^- solution; the lower concentrations give general corrosion, and the higher ones give both pitting and general corrosion simultaneously. The pitting corrosion can occur for various metal alloys both in Cl- only solutions and Cl^- $S_2O_3^{2-}$ solutions. The transition from metastable pit to stable pit formation can be triggered early by the pit escalating with the increase of $S_2O_3^{2-}$. When $S_2O_3^{2-}$ is present, it does not reduce on the passive film itself rather on the defective sites of the passive film. The corrosive effect of $S_2O_3^-$ Cl^- ions on various metal alloys are reported by Wensley et al. [19] that polysulfides and $S_2O_3^{2-}$ can cause a detrimental effect by degrading the passivation ability. $S_2O_3^{2-}$ ions are not corrosive enough when present alone as it does not initiate the breakdown of the passive film, except in Cl^- only solutions and Cl^- $S_2O_3^{2-}$ solutions. When $S_2O_3^{2-}$ concentration equals or exceeds the Cl^- ion concentration, the decrease in current density is observed by K. Baranwal et al. [20] from polarization measurements due to the formation of thicker sulfide layer formed on the metal surface which limits the diffusion of active species. However, there are acquired potential and current density in various ratio Cl^-: $S_2O_3^{2-}$ (Fig 2-13).

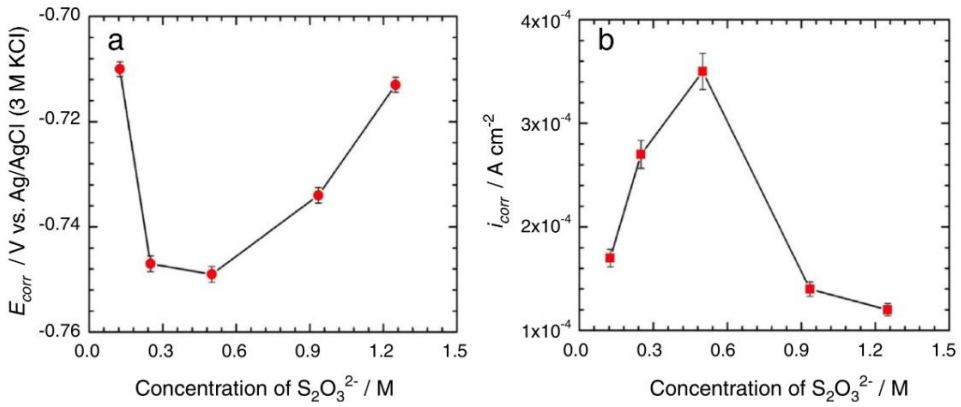

Figure 2-13. E_{corr} (left) and i_{corr} (right) values acquired for various ratio of Cl^-:$S_2O_3^{2-}$ [20]

CHAPTER (3)
EXPERIMENTAL PROCEDURE

This chapter presents the prevention process of passivation on zinc alloys starting from cutting the samples into the desired size for experiments with electric discharge machining (EDM), surface preparation, immersion tests, polarization tests and characterizations. The passivation behaviors of zinc alloys (Z32120 and Z13000) are investigated by potentiodynamic polarization methods followed by the surface characterization with FE-SEM and EDX.

3.1 Experimental Steps

- Materials and Solution Preparations
- Electrochemical Tests
- Surface Characterization
- Data Analysis and Results

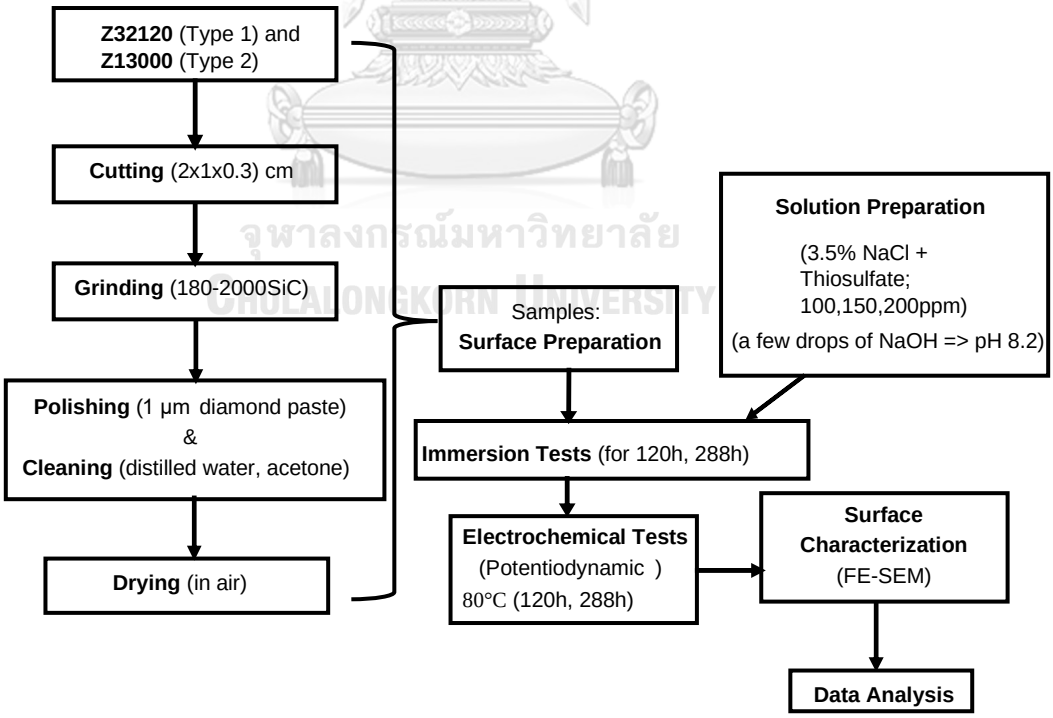

Figure 14-1. Schematic diagram of overall experimental process

3.2 Materials and Solution Preparation

UNS (Unified Numbering System) Type 1 (Z32120) and Type 2 (Z13000) Zn-alloys shown in Table 3-1, which have 0.1-0.5%Al and 0.0005%Al, were used in the research. The alloy samples were cut into the required size (2 x 1 x 0.3 cm) by electric discharge machining (EDM). All samples were ground with silicon carbide papers ranging from No. 80 to 2000, then followed by polishing with 1 μm diamond paste, cleaning carefully with distilled water, acetone and finally, dried in air. The 3.5% NaCl solution (pH 8.2 by a few drops of NaOH) mixed with thiosulfate in the various concentrations of 100ppm, 150ppm and 200ppm, was prepared for both immersion tests and electrochemical tests.

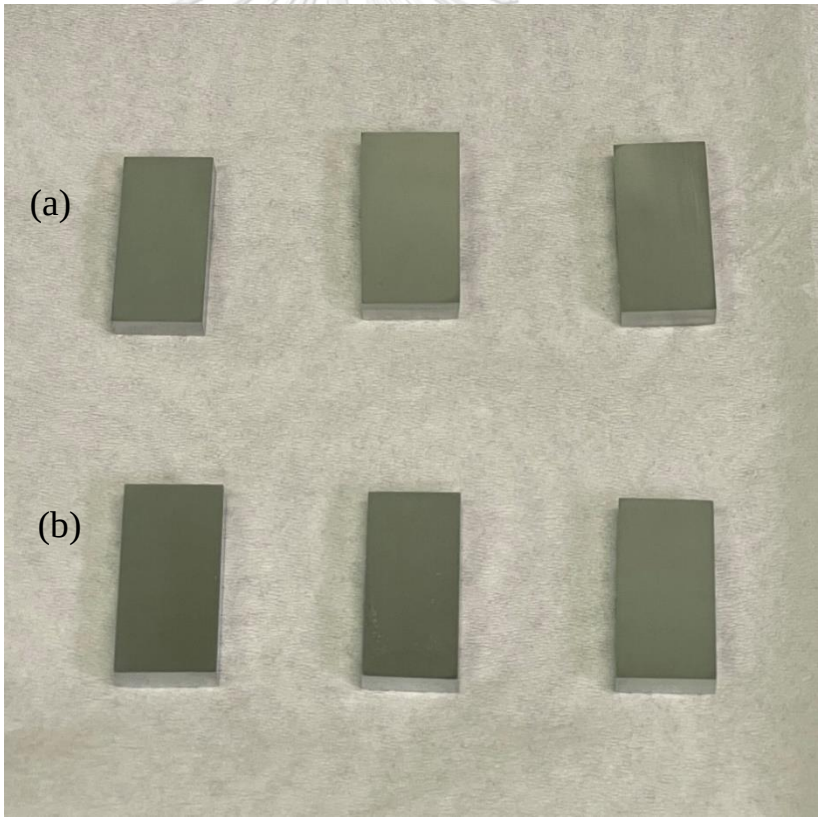

Figure 15-2. Samples prepared for testing; (a) Z32120 and (b) Z13000

Table 5-1. Standard compositions of Zn alloys used for the experiment after ASTM B418

Type (UNS)	Composition (wt.%)						
	Al	Cd	Fe (max)	Pb (max)	Cu (max)	others	Zn
I (Z32120)	0.1-0.5	0.025-0.07	0.005	0.006	0.005	0.1	remain
II(Z13000)	0.005 max	0.003 max	0.0014	0.003	0.002	…..	remain

3.3 Immersion and Electrochemical Tests

3.3.1 Immersion Test

All the samples of both Z32120 and Z13000 Zn-alloys were immersed in 3.5% NaCl solution mixed with thiosulfate for 288h at 80°C. There are 6 conditions of immersion test that involve 2 types of samples in 3 different concentrations. The purpose of the test was to investigate whether the passivation occured in the presence of thiosulfate, or the effect of thiosulfate inhibited the passivation before the potentiodynamic polarization tests compared to the Zn passivation in the absence of thiosulfate from the work of T. Kaewmaneekul et al. in the same temperature and immersion time.

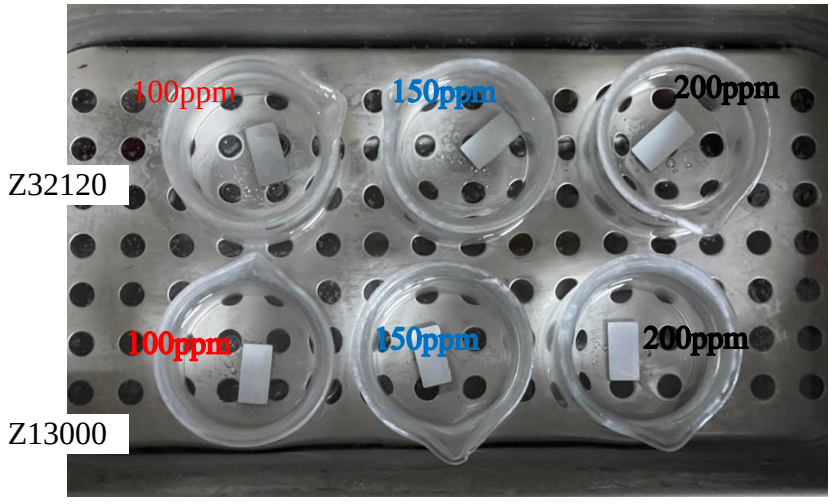

Figure 16-3. Samples immersed in 3.5%NaCl + thiosulfate solutions at 80°C

3.3.2 Potentiodynamic Polarization

The electrochemical tests were conducted using Potentiostat Autolab (Figure 3-2) with a three-electrode cell and run with Nova 1.11 Program. The three-electrode cell (Figure 3-3) contained the test samples as working electrodes, platinum rod as counter electrode and Ag/AgCl electrode as reference electrode. The potentiodynamic polarization curves of the test sample at each period of 1800s were recorded on the surface area of 2.9cm^2 at the applied potentials range of -0.9 to 1 V (vs. Ag/Ag/Cl) with a scan rate of 1mVs^{-1} at the potentiostatic temperature of 80°C. Electrochemical tests were investigated on the 6 conditions of immersion tests and then, followed by recording the pH of the solution. To check reproducibility, all electrochemical measurements were conducted at least twice on one round.

Figure 17-4. Autolab Potentiostat (AUT84437)

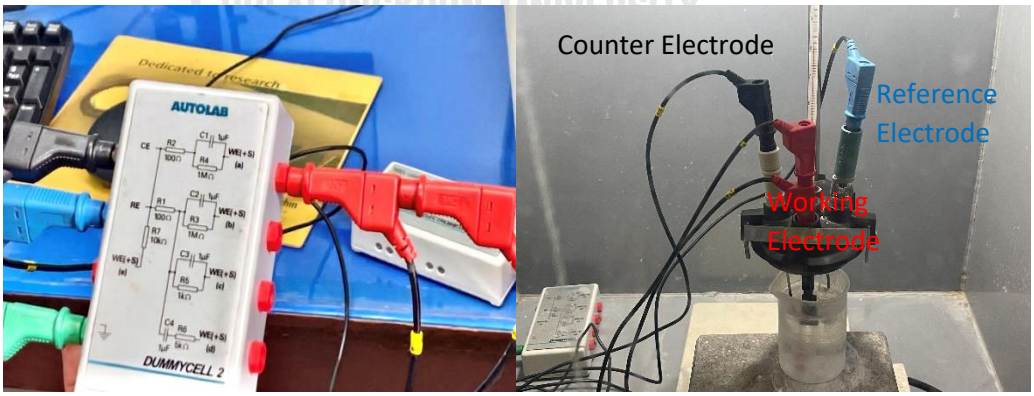

Figure 18-5. Dummy cell (left) and self set-up three-electrode cell (right)

3.4 Surface characterization

The passive film morphology of the samples after anodic polarization from corrosion potentials up to desired potentials was examined using a field emission scanning electron microscope (FE-SEM). The elemental compositions of the film at the same conditions of FE-SEM investigation were evaluated by energy disperse X-ray (EDX). Its computational view can be seen in Figure 3-6.

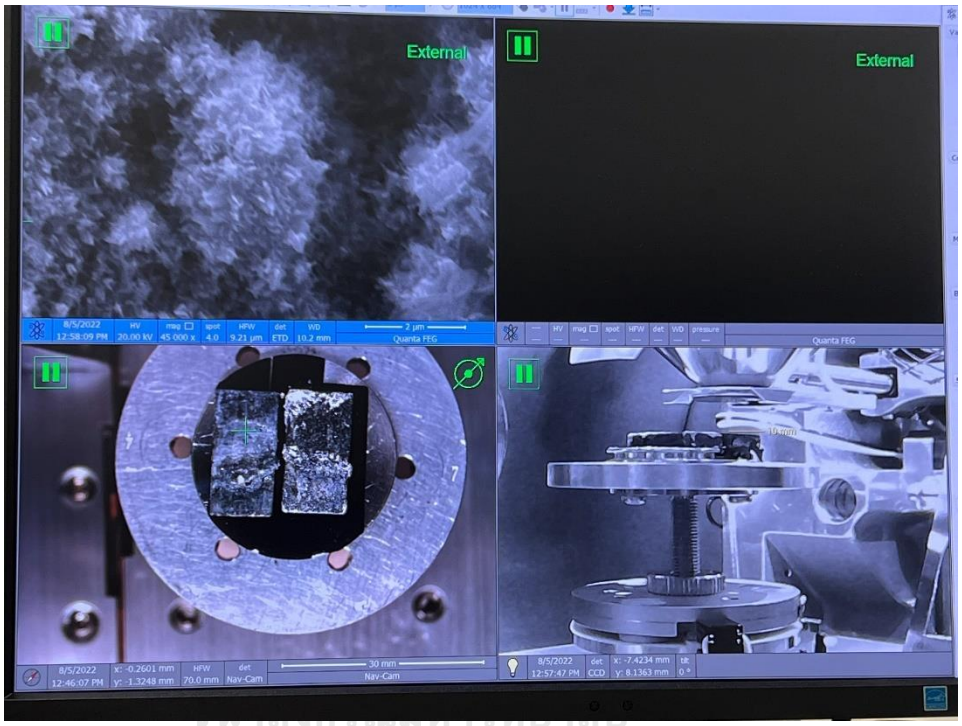

Figure 19-6. Computational view of Field Emission Scanning Electron Microscopy (FE-SEM) (Quanta FEG 250)

CHAPTER (4)
RESULTS AND DISCUSSION

4.1 Electrochemical tests

The electrochemical test done in this work is potentiodynamic polarization. Polarization curves are described with potential and current density. Typically, there are two types of polarization curves that can be found as shown in Figure 4-1.

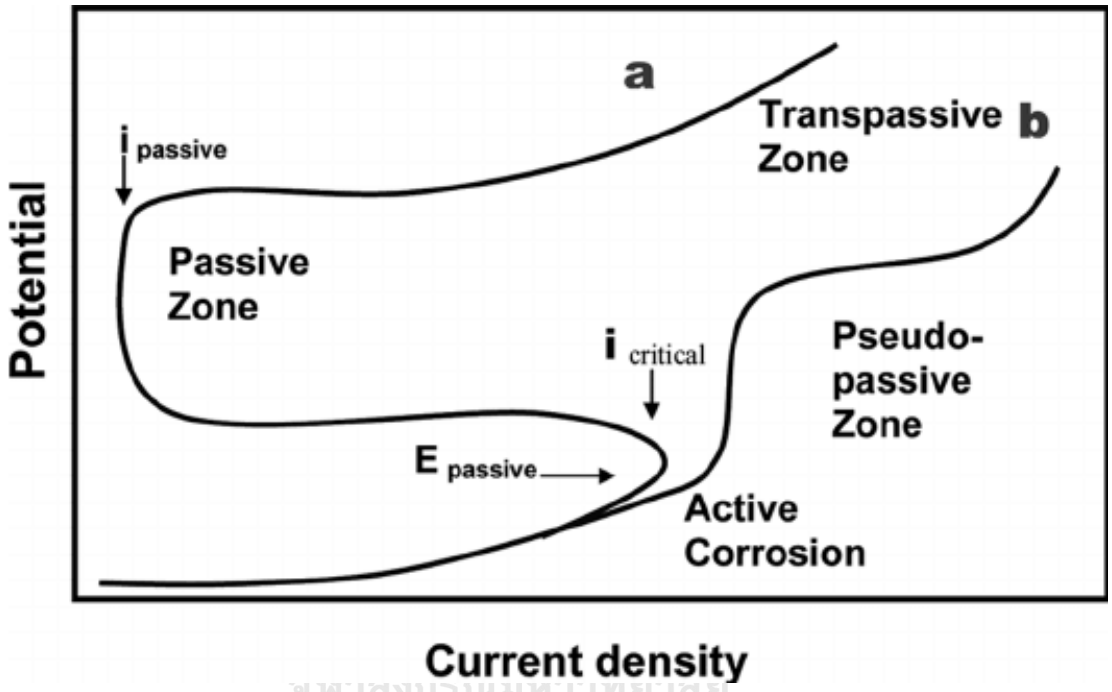

Figure 20-1 Typical polarization curves

4.1.1 Potentiodynamic polarization curves at 120h

The potentiodynamic curves of Zn alloys; Type 1 and Type 2 of immersion in solution with different thiosulfate content (100ppm, 150ppm, 200ppm) for 120h at 80°C are shown in Figure 4-2. The current density values listed in Table 4-1 are the values of the most curved point on the polarization curves. It is found that 150ppm content gives approximately related results in average passive current density (i_{pass}) for both Type 1 and Type 2 in $6.7x10^{-3}$ A/cm^{-2}. However, there are slight differences between 100ppm and 200pp. Type 1 has i_{pass} of $7.1x10^{-3}$ A/cm^{-2} in 100ppm while Type 2 has $6.7x10^{-3}$ A/cm^{-2}, in 100ppm. The average i_{pass} values in 200ppm are different

between Type 1, 7 $x10^{-3}$ A/cm^{-2} and Type 2, 5.9 $x10^{-3}$ A/cm^{-2}. For both alloys, 100ppm gives highest i_{pass}. But 150ppm gives a higher i_{pass} for Type 2 and lower i_{pass} for Type 1, than 200ppm. Type 1 is equal or higher i_{pass} in all thiosulfate content than Type 2. 100ppm and 200ppm for Type 1 are approximately similar in value with 7 $x10^{-3}$ A/cm^{-2}. Also, the same i_{pass} value ($6.7x10^{-3}$ A/cm^{-2}) is measured in 100ppm and 150ppm for Type 2.

Overall, by the i_{pass} values of Zn alloys, it can be said that thiosulfate in the solution is more effective to hinder the passivation of for Type 1 than for Type 2 at 120h at 80°C. However, only poor films are occurred on both alloys because of thiosulfate. The corrosion resistance of passive films on Zn alloys is outstanding with the value at $0.59x10^{-6}$ A/cm^{-2} and unacceptable at over $2x10^{-3}$ A/cm^{-2} [5]. The results of this work have current density values which exceed $2x10^{-3}$ A/cm^{-2} as shown in Table 4-1. Morever, mean ±Standard Deviation (±SD) of the current density values as shown in Table 4-2, also exceed $2x10^{-3}$ A/cm^{-2}. Therefore, it can be said that thiosulfate retards the passivation with the almost same amount of effect for both Type 1 and Type 2 in such conditions.

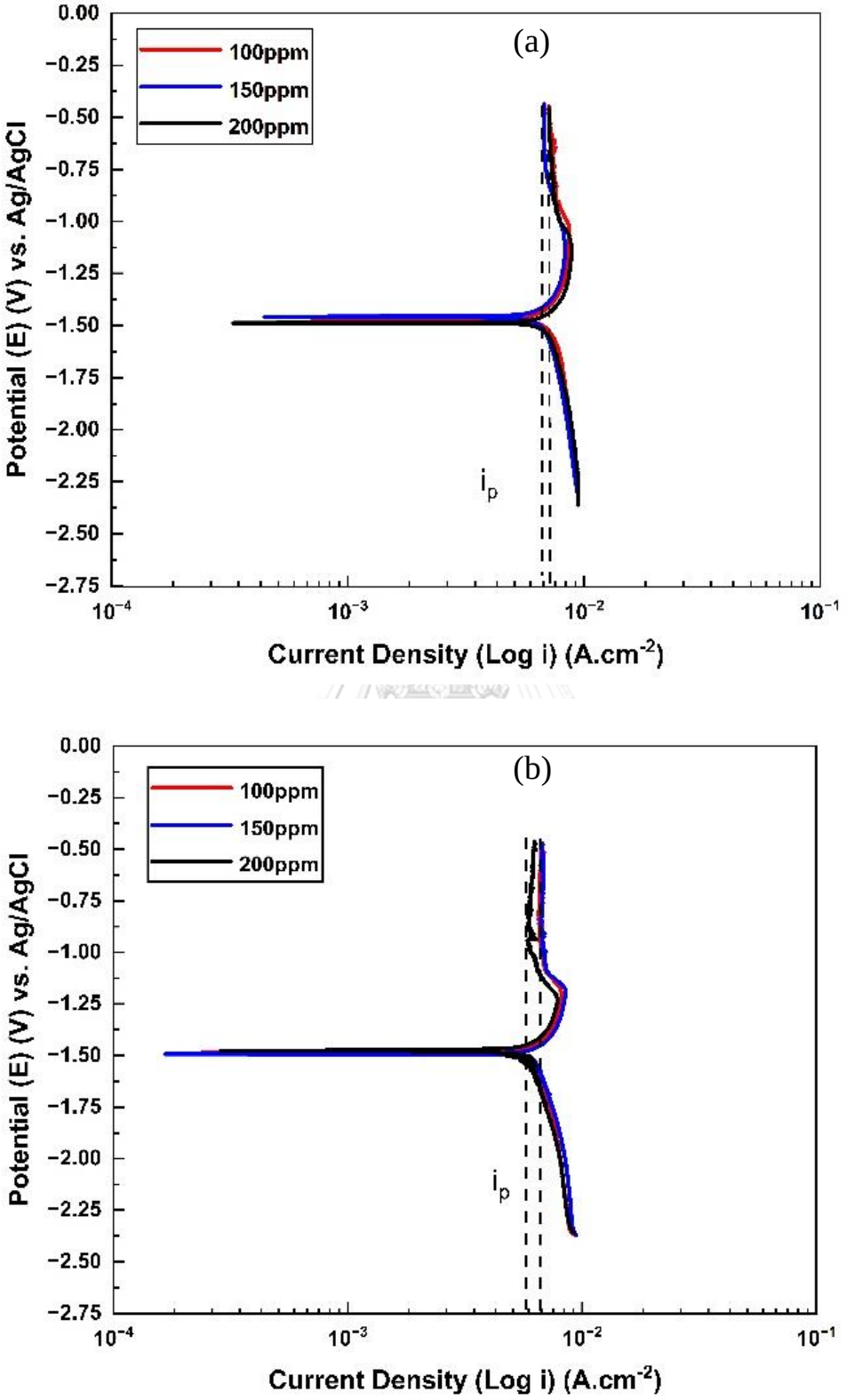

Figure 21-2. Potentiodynamic polarization curves at 120h of (a) Type 1 and (b) Type 2, in 3.5 wt.% NaCl with different thiosulfate concentrations.

Table 6-1. Passive current density values of Type 1 and Type 2 measured on the most curved points of all thiosulfate concentrations at 120h

Samples	100ppm (A/cm^{-2})	150ppm (A/cm^{-2})	200ppm (A/cm^{-2})
Type 1 (Z32120)	$7.1x10^{-3}$	$6.7x10^{-3}$	$7 x10^{-3}$
Type 2 (Z13000)	$6.7x10^{-3}$	$6.7x10^{-3}$	$5.9 x10^{-3}$

Table 7-2. Standard deviations of passive current densities of Type 1 and Type 2 in 100ppm, 150ppm, 200ppm (120h, 80 °C)

Type 1 (Z13000) Data	**N total**	**Mean (A/cm^{-2})**	**Standard Deviation (±SD) (A/cm^{-2})**	**Sum**	**Minimum**	**Median**	**Maximum**
[100ppm120h] [825:1779]	955	0.00736	6.88243E-4	7.02532	0.00215	0.00729	0.0083
[150ppm120h] [822:1779]	958	0.00734	7.80045E-4	7.02762	4.43848E-4	0.00729	0.0083
[200ppm120h] 819:1779]	961	0.00773	7.92153E-4	7.43107	3.26843E-4	0.00751	0.00885
Type 2 (Z32120) Data	**N total**	**Mean (A/cm^{-2})**	**Standard Deviation (±SD) (A/cm^{-2})**	**Sum**	**Minimum**	**Median**	**Maximum**
[100ppm120h] [831:1779]	949	0.00694	7.1575E-4	6.58665	2.38373E-4	0.00668	0.00816
[150ppm120h] [825:1779]	955	0.00713	7.42343E-4	6.81269	1.66107E-4	0.00681	0.00849
[200ppm120h] [829:1779]	951	0.00644	7.70378E-4	6.12031	2.86407E-4	0.00618	0.00785

4.1.2 Potentiodynamic polarization curves at 288h

At 288h, the effect of thiosulfate still inhibits the passivation shown in Figure 4-3, just as same as at 120h after the immersion time is doubled up. The current density values listed in Table 4-4 are also the values of the most curved points on the polarization curve. In 150ppm of thiosulfate, both alloys have an average i_{pass} of $7.6x10^{-3}$ A/cm^{-2}. This same i_{pass} value by 150ppm for both alloys is between the i_{pass} of Type 2 in 100ppm ($7x10^{-3}$ A/cm^{-2}) and the i_{pass} of Type 1 in 200ppm ($7.9 x10^{-3}$ A/cm^{-2}). The lowest values of i_{pass} respectively measured to be $5.6 x10^{-3}$ A/cm^{-2} for Type 1 in 100ppm and $6.2 x10^{-3}$ A/cm^{-2} for Type 2 in 200ppm, indicates that the tendency of passivation growth is more likely to happen if the immersion time is longer. Despite these two thiosulfate contents for respective alloys for passivation growth, the other contents such as 150ppm and 200ppm for Type 1 and 100ppm and 150ppm for Type 2, increase in i_{pass} values with respect to the longer immersion time. Also, both the current density values of the most curved points and the values (Mean ± Standard Deviation) in Table 4-4, exceed the typical current density value ($2x10^{-3}$ A/cm^{-2}) of unacceptable passive film.

Type 2 has the hindrance of passivation by all thiosulfate concentrations in the solutions. The same generates for Type 1 in all concentrations and however, the exception is 100ppm that got lower in i_{pass} value at 288h compared to the higher value at 120h which led to the passivation growth in the increasing time. Therefore, it is found that lower concentration of thiosulfate into the solution with longer immersion time, leads for the passivation growing the poor film to the richer one for Type 1 and higher concentration leads for the passivation with increasing time for Type 2.

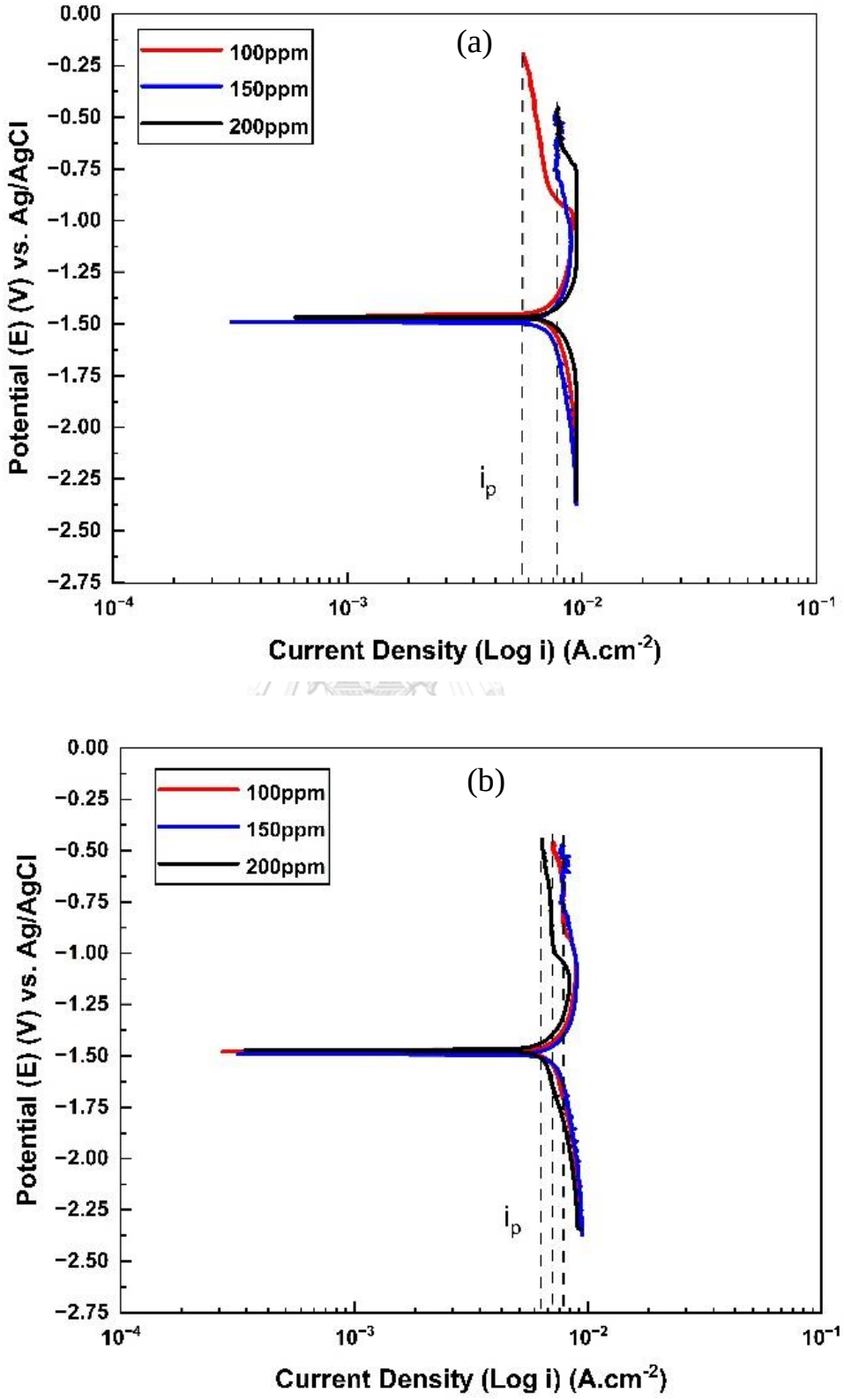

Figure 22-3. Potentiodynamic polarization curves at 288h of (a) Type 1 and (b) Type 2, in 3.5 wt.% NaCl with different thiosulfate concentrations.

Table 8-3. Passive current density values of Type 1 and Type 2 measured on the most curved points of all thiosulfate concentrations at 288h

Samples	100ppm (A/cm^{-2})	150ppm (A/cm^{-2})	200ppm (A/cm^{-2})
Type 1 (Z32120)	$5.6x10^{-3}$	$7.6x10^{-3}$	$7\ x10^{-3}$
Type 2 (Z13000)	$7x10^{-3}$	$7.6x10^{-3}$	$6.2\ x10^{-3}$

Table 9-4. Standard deviations of passive current densities of Type 1 and Type 2 in 100ppm, 150ppm, 200ppm (288h, 80 °C)

Type 1 (Z13000) Data	**N total**	**Mean (A/cm^{-2})**	**Standard Deviation (±SD) (A/cm^{-2})**	**Sum**	**Minimum**	**Median**	**Maximum**
[100ppm288h] [596:1779]	1184	0.00735	0.00118	8.7011	0.00121	0.00703	0.00911
[150ppm288h] [826:1779]	954	0.00821	6.93673E-4	7.83315	3.18207E-4	0.00825	0.00897
[200ppm288h] [828:1779]	952	0.00889	7.91015E-4	8.45952	5.95856E-4	0.00939	0.00947
Type 2 (Z13000) Data	**N total**	**Mean (A/cm^{-2})**	**Standard Deviation (±SD) (A/cm^{-2})**	**Sum**	**Minimum**	**Median**	**Maximum**
[100ppm288h] [826:1779]	954	0.00801	7.51713E-4	7.63887	2.73254E-4	0.00788	0.0089
[150ppm288h] [826:1779]	954	0.00821	6.93673E-4	7.83315	3.18207E-4	0.00825	0.00897
[200ppm288h] [819:1779]	961	0.00718	7.76488E-4	6.90438	3.39325E-4	0.00699	0.00835

4.2 Characteristics of surfaces

4.2.1 Morphologies

FE-SEM micrographs for Type 1 and Type 2 after anodic polarization in solutions with different thiosulfate concentrations are shown in Figure 4-4 and Figure 4-5. Both alloys have white layer morphologies on the surfaces. Since the potentiodynamic curves of both alloys are shown to have no passivation in Figure 4-2 and Figure 4-3, the white layers seem to be porous and poor adhesion on the surfaces, due to the results of Kaewmaneekul et. al [1]. The surfaces are covered with the uneven depositions of zinc salts or oxides in the form of tangled belts and dendrites morphologies which can increase the specific surface area of the anode facilitating zinc corrosion by causing short circuit between the anode and cathode [21, 22].

Kaewmaneekul et. al [1] showed in the research that the tangled morphologies distributing less uniformly, were effected by Al content related with Cl^- penetration and the immersion time. Also, Zn phases can be reduced by Al increase, having coarse dendritic structures, leading to less corrosion resistance of the metal surface [23]. The microstructures of both alloys also exhibits the uneven surfaces distributing less uniformly due to the random heterogeneous slower nucleation leading to poorer grain boundaries [24]. Therefore, it is clear that the passivation does not occur because of Al related to Cl^-, immersion time and also because of thiosulfate which accelerates the Cl- to have the passive film breakdown [2, 4, 19, 20].

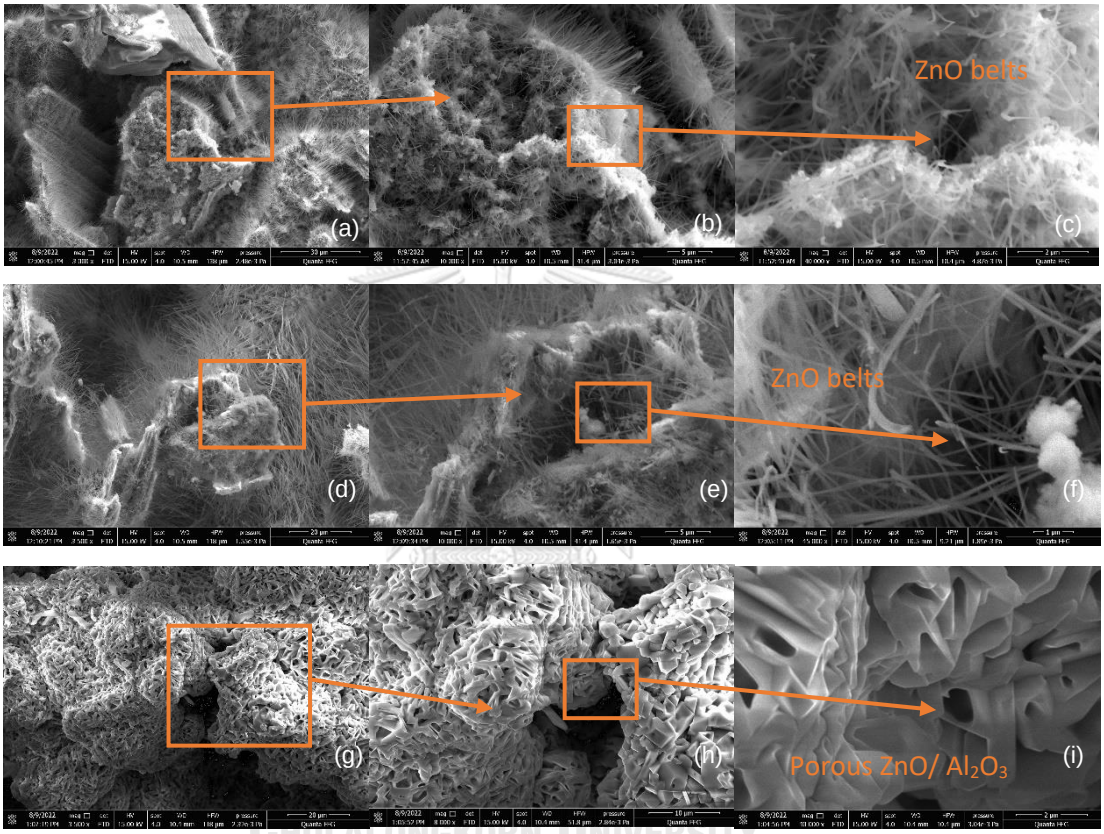

Figure 23-4. FE-SEM micrograph of oxides formed on Type 1 after anodic polarization at 288h in solution with thiosulfate, (a-c) 100ppm, (d-f) 150ppm, (g-i) 200ppm

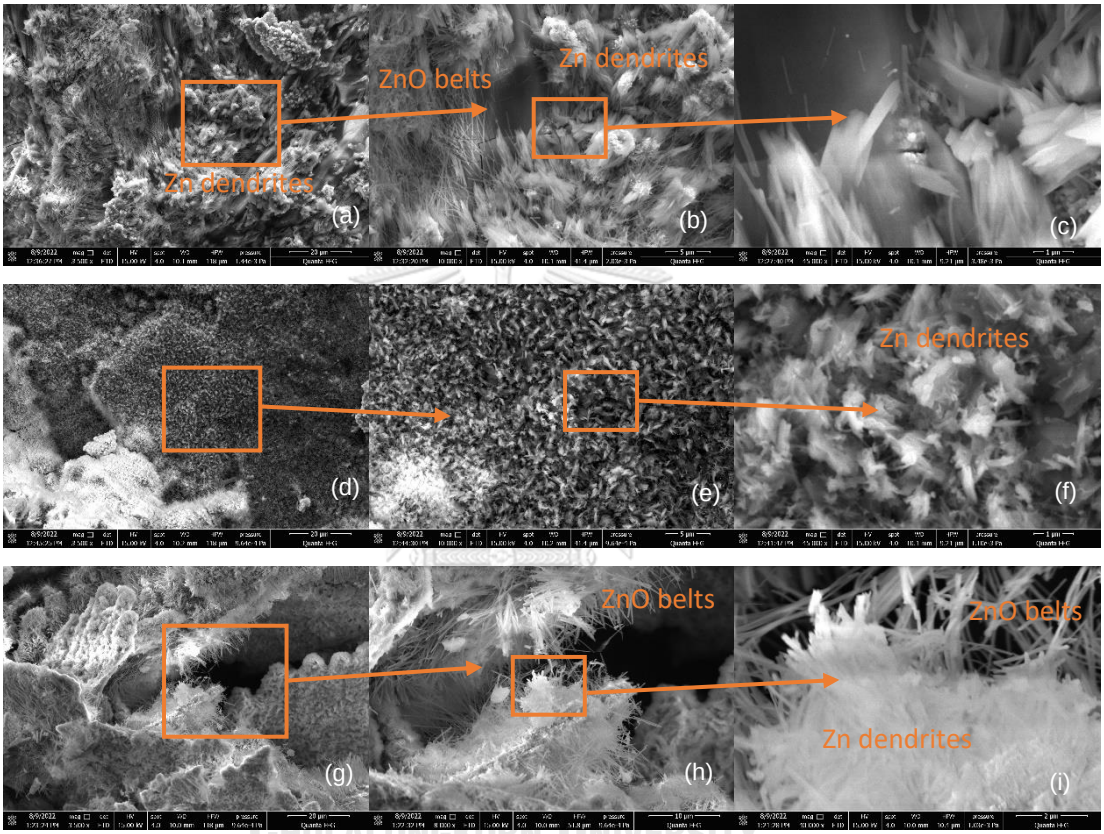

Figure 24-5. FE-SEM micrograph of oxides formed on Type 2 after anodic polarization at 288h in solution with thiosulfate, (a-c) 100ppm, (d-f) 150ppm, (g-i) 200ppm

4.2.2 Surface compositions

The elemental compositions found on the alloys' surfaces by EDX are shown relevantly with the related thiosulfate concentrations in Figure 4-4 and Figure 4-5 on the scale of lowest and highest magnifications. Type 1 contains Al content and Type 2 has Al in very low contents which is nearly regarded as pure Zn.

Because of the white layers, both alloys seem to have zinc salts on the surfaces with respect to the EDX results shown Figure 4-6 and 4-7. Major constituents found significantly in all samples are Zn, O, Cl and Na. Communally, both Type 1 and Type 2 have the zinc salts compounds in the presence of Zn such as ZnO, $Zn(OH)_2$, ZnS, $ZnCl_2$, ZnOHCl, $Zn_5(CO_3)_2(OH)_6$, $Zn_5(OH)_8Cl_2.H_2O$, $Zn_4SO_4(OH)_6.4H_2O$, Zn_4SiO_4, $Zn(CH_3CO_2)_2$, $Zn_5(OH)_8Cl_2$, $Zn(CH_3CO_2)_2$, $Zn(CH_3CO_2)_2.2H_2O$, $Zn_4Si_2O_7(OH)_2.H_2O$, $Zn_5(OH)_8Cl_2.4H_2O$ and $Zn_{12}(OH)_{15}(SO_4)_3Cl_3.5H_2O$ [1, 22, 25].

However, Type 1 with Al exhibits the minor constituents of γ-AlOOH and β-$Al(OH)_3$ which later lead to become $AlCl_3$ after reacting with Cl^- [1], and it is found that Al only in the EDX spectrum of the sample which was tested in 100ppm of thiosulfate. That means Cl^- ions are less in content to react with Al in 100ppm, therefore, leading some of Al to form Al_2O_3 passive film due to the lower concentration of thiosulfate being unable to produce enough Cl^- ions.

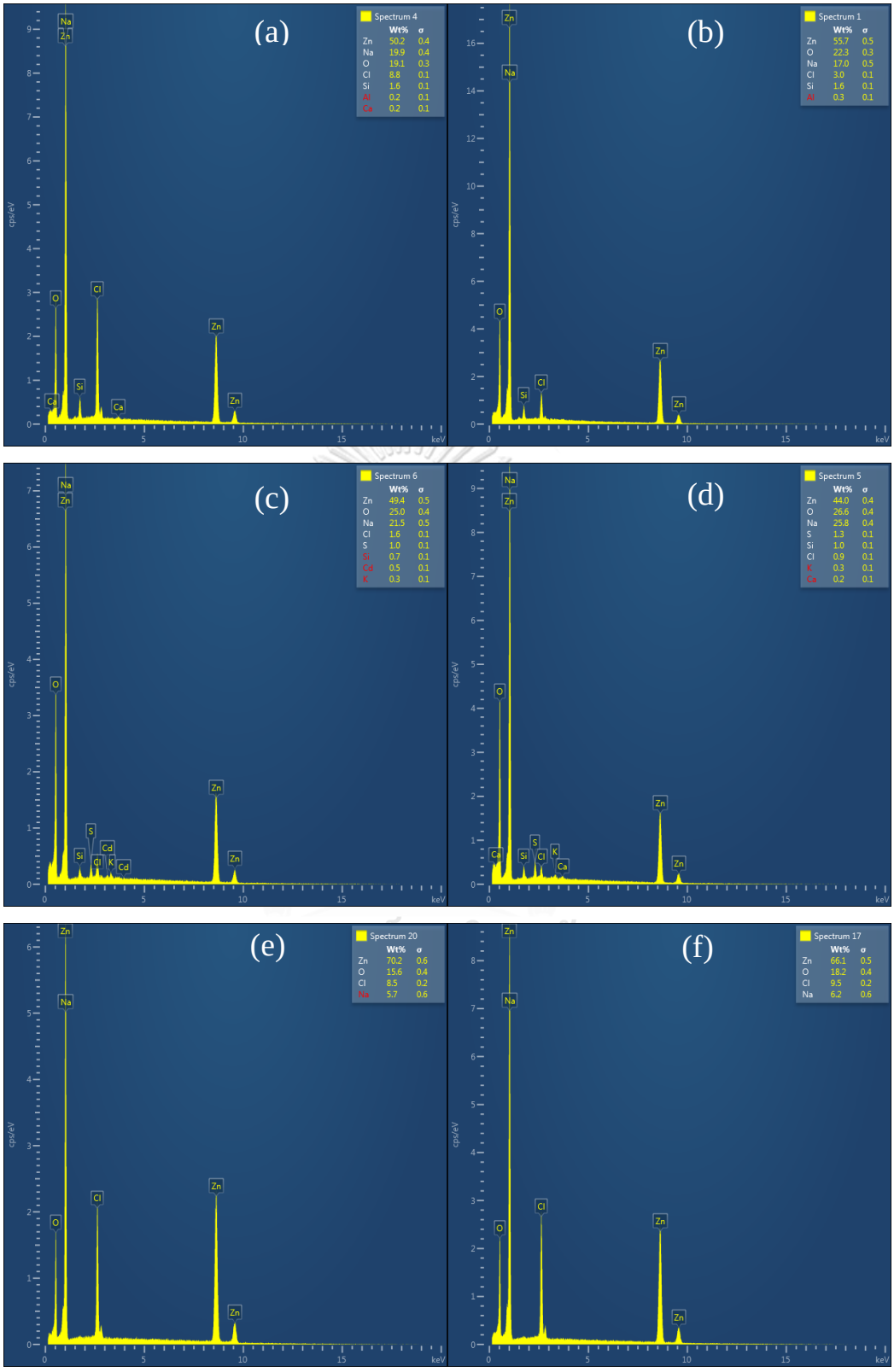

Figure 25-6. EDX on FE-SEM micrograph of Type 1 in lowest and highest magnifications: (a, b) 100ppm, (c, d) 150ppm, (e, f) 200ppm

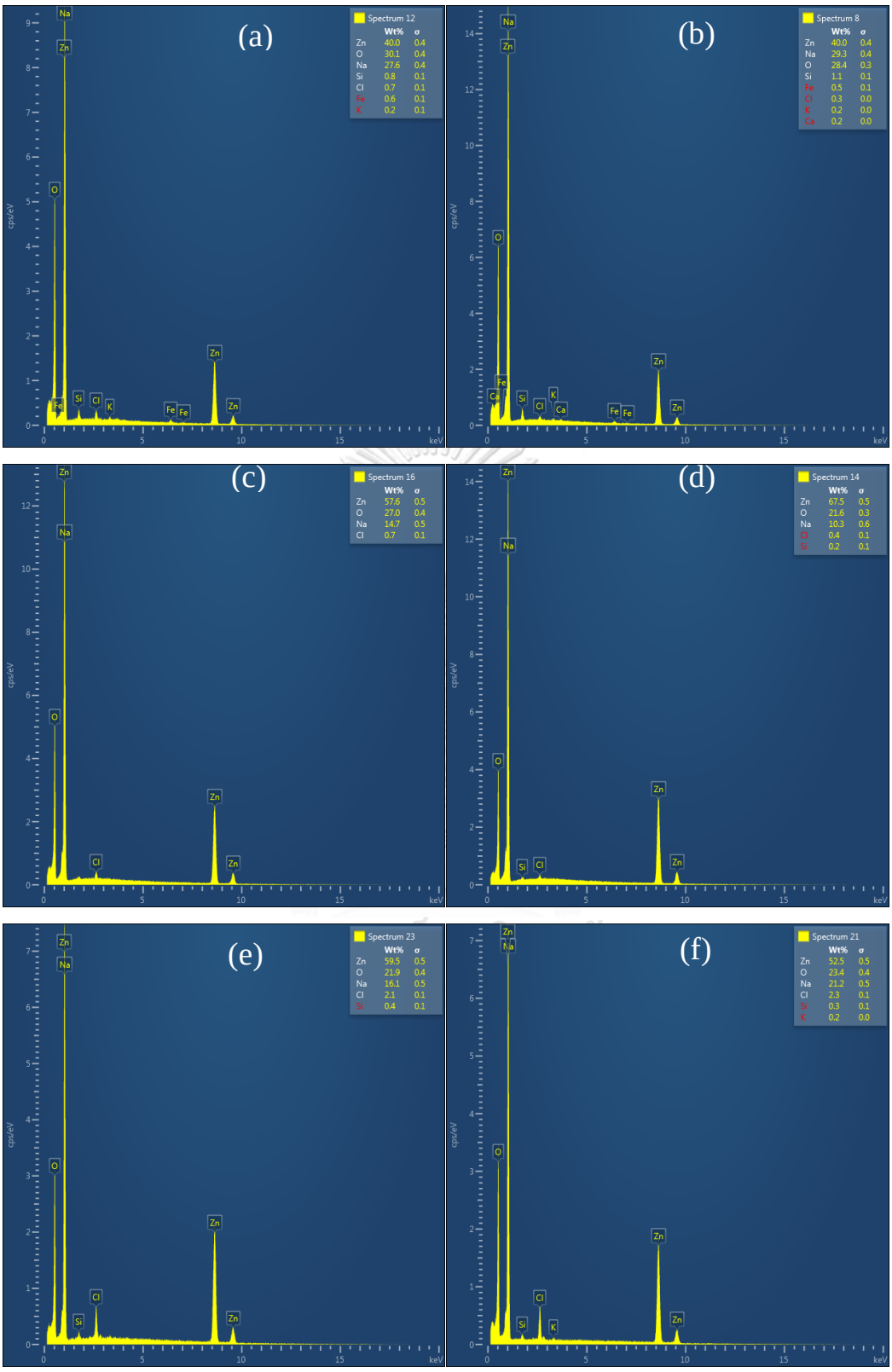

Figure 26-7. EDX on FE-SEM micrograph of Type 2 in lowest and highest magnifications: (a, b) 100ppm, (c, d) 150ppm, (e, f) 200ppm lowest magnification

4.3 Discussion

In this study, both Zn alloys, Type 1 and Type 2 can make the passivation not to occur or occur with poor passive film in 3.5% NaCl solution at 80°C by the effect of thiosulfate adding in the solution. The effect of thiosulfate is discussed based on the results of potentiodynamic polarization and FE-SEM with EDX as follows:

4.3.1 Effect of immersion time

When Zn alloys have passivation and then generate depassivation during an immersion test, how long the immersion throughout the process is significant. In the ranging from 120h to 288h, passivation occurs on Zn alloys by the proof of T. Kaewmaneekul et. Al [1]. Nonetheless, those Zn alloys are similar to the ones that were tested in this work and then it happens to be no passivation with the same immersion time intervals. Typically about the passivation, passive films are phenomenal at the current density value of $0.59x10^{-6}$ A/cm^{-2} and they are undesirable starting from $2x10^{-3}$ A/cm^{-2} [5]. According to this study, passivation is undesired, therefore, the passive current density values need to be equal to or greater than $2x10^{-3}$ A/cm^{-2}. Figures 4-2 and 4-3 exhibit passive current density values that are greater than $2x10^{-3}$ A/cm^{-2}. The difference between T. Kaewmaneekul [1] this work is the environment which Zn alloys are immersed in depending on the absence of thiosulfate and its presence. However, in this work, the time of immersion is found to be rarely effective, and it could be ineffective with the presence of thiosulfate in the solution although the solution pH changed in the gradual decrease as the increase of immersion time. Hence, immersion time affects Zn alloys differently based on the environment.

4.3.2 The change of pH at 80°C

Immersion tests and electrochemical tests were conducted at the same temperature of 80°C as same as T. Kaewmaneekul [1]. The solution pH started with 8.2 at 0h before the samples were put into the water bath and it rose to 10.3 after putting the samples into water bath for 0.5h at 80°C. Each 24h, the pH values change with ±1 or ±2 between each interval as shown in Table 4-3 and Table 4-4. This is because OH^- ions content was more in the solution than H^+ ions causing the solution to be basic instead of acidic.

The cause was the water dissociation (self-ionization) which employs both for pure water and any aqueous solution [26]. This ionization is generated by the proton (H^+) loss, i.e. deprotonation as shown in Figure 4-8, to form and leave OH^- (hydroxide ion) behind spontaneously as H^+ immediately protonates with companion water molecule to result H_3O^+ (hydronium ion) [26-28]. When water is heated, the dynamic equilibrium between water and its ions is interrupted. The reverse reaction of water ionization on the left side of equilibrium is increased by the applied heat because the reverse ionization of water is exothermic, and the reaction rate increases.

According to LeChatellier's principle, if the temperature increases, the equilibrium will shift towards the endothermic reaction which is heat absorption. The reaction will go as Figure 4-8, shifting the equilibrium to the forward (right) direction for the purpose of countering the heat supply by speeding up the endothermic reaction to generate huge amounts of OH^-, H^+ and H_3O^+. Hence, to summarize, those kinds of water ions increase with the increased temperature that causes water to be hot.

Moreover, water molecule is both amphiprotic and amphoteric, both of which means that molecules or ions can either donate or accept a proton depending on the circumstances and also means that they can act as either acid or base [26]. According to the Bronsted-Lowry theory, in the reaction of acid and base, the acid forms its conjugate base donating the proton and the base forms its conjugate acid accepting the proton. This is known as dissociation of acid in water in the general formula [29] as:

$$HA + H_2O \leftrightarrow H_3O^+ + A^- \quad (14)$$

Thus, in Figure 4-8, one water molecule among two water molecules, donates proton to another one which acts as base to become the conjugate acid, leaving the donator water molecule to result as the conjugate base [26, 29]. H_3O^+ is conjugate acid resulted from the water molecule which acts as base [29]. If $[H_3O^+]$ is greater than $[OH^-]$, the solution is acidic and oppositely, the solution is basic. In this work, as the solution pH resulted to be 10.3 after 0.5h, OH^- content is greater in the solution than H_3O^+. Nonetheless, all solutions utilized in this study decreased steadily and slowly with the increasing time of immersion at 80°C.

Table 10-3. pH measurements per 24h on solutions immersed of Type 1 (Z32120)

Hour (h)	100ppm	150ppm	200ppm
24	10.3	10.3	10.2
48	10.2	10.3	10.2
72	10.2	10.2	10.2
96	10.2	10.2	10.1
120	10.3	10.2	10.2
144	10.2	10.1	10.1
168	10.1	10.2	10.2
192	10.2	10.2	10
216	10.1	10.2	10.1
240	9.9	10	10
264	9.8	10	9.9
288	9.8	9.9	9.9

Table 11-4. pH measurements per 24h on solutions immersed of Type 2 (Z13000)

Hour (h)	100ppm	150ppm	200ppm
24	10.2	10.2	10.3
48	10.1	10.2	10.1
72	10.1	10.2	10.2
96	10.1	10.1	10.1
120	10.2	10.2	10.2
144	10.1	10.1	10.1
168	10	10	10.1
192	10.1	10	10.1
216	9.9	10	10.1
240	10	9.9	10
264	10	10	9.9
288	9.9	9.9	10

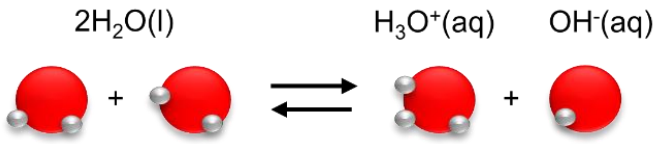

Figure 27-8. Water molecules dissociation by self-ionization

4.3.3 Surface morphology by pH and temperature

Due to the greater content of OH^- in solutions immersed samples, most of the ions which dissociated within the solutions seems to react with OH^- ions more.

Typically, corrosion product such as zinc hydroxide ($Zn(OH)_2$) formed from aqueous solution at room temperature. It would have greater solubility at elevated temperature and later transformed into the imperfect zinc oxide (ZnO) [14]. The heavy metal compounds such as oxides, hydroxides, and carbonates, are soluble respectively with the pH value. The lower the pH, the more leaching of cations and oppositely the more anions leaching, the higher pH [30, 31]. The solutions pH in this work is preserved around 10 due to the presence of thiosulfate, anions (Cl^-, OH^-, S^-) leaching is likely to be higher than that of cations (Zn^{2+}, Al^{3+}, Fe^{2+}, Cd^{2+} and Cu^{2+}). Within pH 7 and 10, the cations and heavy metals such as Zn leaches in the least amount, shown in Figure 4-9.

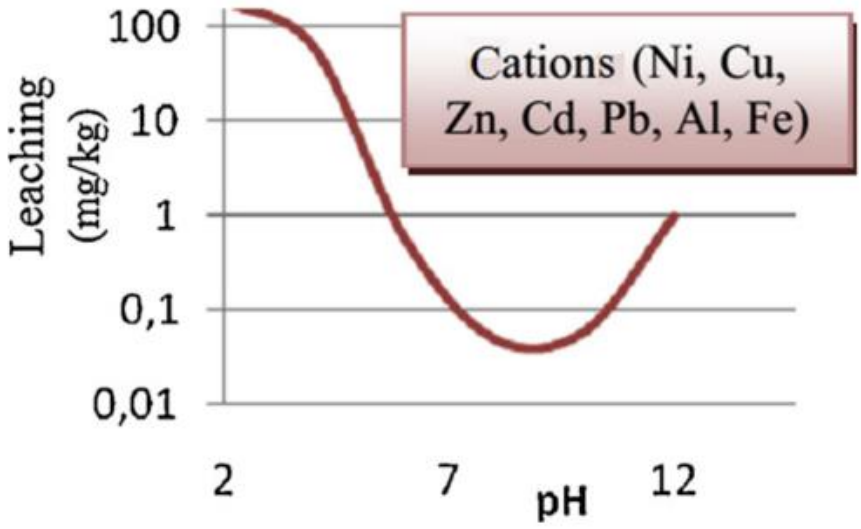

Figure 28-9. The general diagram of leaching cations and anions by pH[30]

Zn precipitates mostly $ZnCl_2$, $Zn(OH)_2$ and ZnO in alkaline solution over pH 8 containing modest amount of Cl^- content [25, 31]. ZnO is resulted from $Zn(OH)_2$ and has buffer layer like ZnS [32]. The successive reactions of ZnO were already shown in Equation (5) to Equation (7) in section 2.6 [1]:

$$Zn \rightarrow Zn^{2+} + 2e^- \quad (5)$$

$$Zn^{2+} + 2OH^- \rightarrow Zn(OH)_2 \quad (6)$$

$$Zn(OH)_2 \rightarrow ZnO + H_2O \quad (7)$$

The formation of $ZnCl_2$ is led by the combination of hydronium ion with Cl^- containing HCl which later would combine with Zn leading to the occurrence of H_2 or H_2S, as shown in Equation (15) to Equation (17) [26]:

$$H_3O^+ + Cl^- \rightarrow H_2O + HCl \quad (15)$$

$$Zn + 2HCl \rightarrow ZnCl_2 + H_2 \quad (16)$$

$$Zn + 2HCl \rightarrow ZnCl_2 + H_2S \quad (17)$$

ZnS is formed from elemental sulfur (S^0) or sulfide (S^{2-}) decomposed from thiosulfate ($S_2O_3^{2-}$) [33]. It is generally shown as Equation (18):

$$Zn + S \rightarrow ZnS \quad (18)$$

At pH 10, ZnS appears to be thickest with porous structure as Al_2O_3 [32, 34]. The higher the pH is, the more OH^- in the solution combining with Zn which is of not enough amount to form ZnS [32]. Thus, ZnS, $Zn(OH)_2$, $ZnCl_2$ and Al_2O_3 are likely to be present typically on both types of Zn alloys in this work, and it is because of the thiosulfate effect.

4.3.4 Effect of thiosulfate

Thiosulfate ($S_2O_3^{2-}$) is well known for its corrosive effect and that effect can be promoted by the inhibition reactions between sulfite and oxygen which depends on the ratio of sulfite and thiosulfate [3, 15, 16]. The corrosion rate in a solution is higher with thiosulfate than the solution without it. General corrosion induced by Cl^-, is accelerated with the increase of $S_2O_3^{2-}$ concentration [3, 4, 17, 18].

Thiosulfate is thermodynamically stable only in the neutral and alkaline solutions tending to undergo chemical decomposition reducing to elemental sulfur (S^0) and sulfide (S^{2-}) [11, 35, 36]. The reduction of $S_2O_3^{2-}$ deduct the H^+ content leading pH

decrease on the metal surface, especially under high corrosion conditions [3]. As shown in Pourbaix diagram, Figure 4-10 [11], if the pH is above 7, $S_2O_3^{2-}$ likely to result the dissolved bisulfide (HS^-) from elemental sulfur (S^0) by the disproportionation with the temperature increase and thereby , that phenomenon tends to be the catalyst of Fe dissolution in alkaline solution [36, 37]. Therefore, as the solution pH in this work was around 10, Fe dissolution is considered to take place on the samples.

The coexistence of thiosulfate with Cl^- promotes localized corrosion even by the small amount in the solution. However, thiosulfate alone rather assists Cl^- ions to initiate pitting sites by breaking down the passive film than attacks the pitting. Hence, the decrease of stable pits survival can depend on their ratio [4, 37]. That is why the Cl-: $S_2O_3^{2-}$ ratio is significant on passivation.

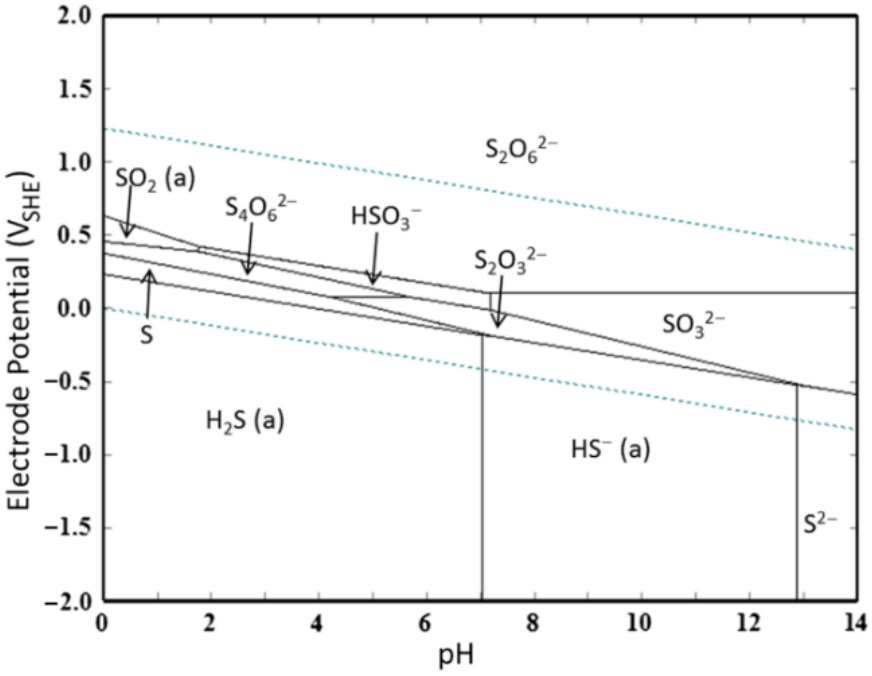

Figure 29-10. Pourbiax diagram for S-H_2O system at 298K[11]

4.3.5 Effect of thiosulfate with Cl^-

The Cl^-:$S_2O_3^{2-}$ ratio plays a key role in Cl^- solution by enhancing the metal pitting and dissolution of the oxide films [20]. The potential of pit in any solution can drop down as the temperature increase according to the Cl^-:$S_2O_3^{2-}$ ratio increasing [11].

Therefore, it is clear that temperature affects not only the dissolving of $S_2O_3^{2-}$ in the solution but also the Cl^-: $S_2O_3^{2-}$ ratio change.

When the $S_2O_3^{2-}$ concentration is greater than or equal to Cl^- ions, the current density decreases limiting the diffusive species by the thick sulfide layers formation on the surface [20]. Apart from Fe, the Zn alloys utilized for this work include the heavy metals such as Cd, Cu and Pb. They all can form sulfide layers by reacting with the dissolved sulfur on the surface. Out of those sulfide layers, only both ZnS and FeS will primarily attack to the alloys in an aggressive way.

The photo-generated holes can oxidize the metal sulfides by photo corrosion [34] Therefore, ZnS and FeS are susceptible to the thermodynamically highly favored oxidation and it is the process which impairs the use of ZnS and FeS due to being photocatalyst (loss of activity and darkening the surface [34, 38]. The sulfide layers formed by the reduction of $S_2O_3^{2-}$ to sulfur is more to happen on the non-protective surfaces [20]. The absorbed elemental actively block OH- ions to diffuse [4].

A small anodic over potential of Al can accelerate the dissolution by the Cl^- presence depolarizing the surface due to the water soluble species [39]. The coexistence of Al and Cl^- operates to get $AlCl_3$ which break the passive film with the Cl^- penetration [1, 40]. $AlCl_3$ is originally formed the dissolved Al which causes Al_2O_3 hydrolysis leading to γ- AlOOH , later transforming into α-$Al(OH)_3$ and β-$Al(OH)_3$. The reactions from Equation (19) to Equation (22) will show the $Al(OH)_3$ formation [1].

$$Al \rightarrow Al^{3+} + 3e^- \quad (19)$$

$$2Al^{3+} + 3H_2O \rightarrow Al_2O_3 + 6H^+ \quad (20)$$

$$Al_2O_3 + H_2O \rightarrow 2AlOOH \quad (21)$$

$$Al_2O_3 + 3H_2O \rightarrow 2Al(OH)_3 \quad (22)$$

Alternatively, Al can directly combine with OH^- to get $Al(OH)_3$ as shown in Equation (23) [40]:

$$Al + 3OH^- \rightarrow Al(OH)_3 + 3e^- \quad (23)$$

$Al(OH)_3$ combines with Cl^- , together penetrating the passive film to transform $AlCl_3$ of which the consecutive reactions are shown in Equation (24) to Equation (26) [40]:

$$Al(OH)_3 + Cl^- \rightarrow Al(OH)_2Cl + OH^- \quad (24)$$

$$Al(OH)_2Cl+Cl^- \rightarrow Al(OH)_2Cl+OH^- \quad (25)$$

$$Al(OH)_2Cl+Cl^- \rightarrow AlCl_3+OH^- \quad (26)$$

The more $S_2O_3^{2-}$ concentration, the faster the sulfide layer formation which leads to the sulfide passivation on the surfaces of alloys. The utilized Zn alloys for this experiment are likely to possess this kind of sulfide passivation according to the measured current density values.

When Type 1 (Z32120) with Al content is immersed in the 3.5% NaCl solution with 100ppm thiosulfate, the current density value dropped within the immersion time of120h and 288h. At the anodic curve side, the current density value of 100ppm shifts towards the more negative values within the 1800s testing time.. The current density value at 288h is lower than the value at 120h. That is proving that Type 1 is gradually forming the passive film in 100ppm thiosulfate. Type 2 (Z13000) with almost no Al content (i.e. literally pure Zn), increase in passive current density at 288h. Despite that, it also tends to act on shifting as similar as Type 1 in 100ppm. If the test time was done longer, the current density of Type 2 immersed in 200ppm could gradually decrease more till it passes the value measured at 120h. The possible oxide layers formed on both alloys by the respective thiosulfate concentration in the solution, which is exposed with both alloys as mentioned above, are illustrated in Figure 4-11.

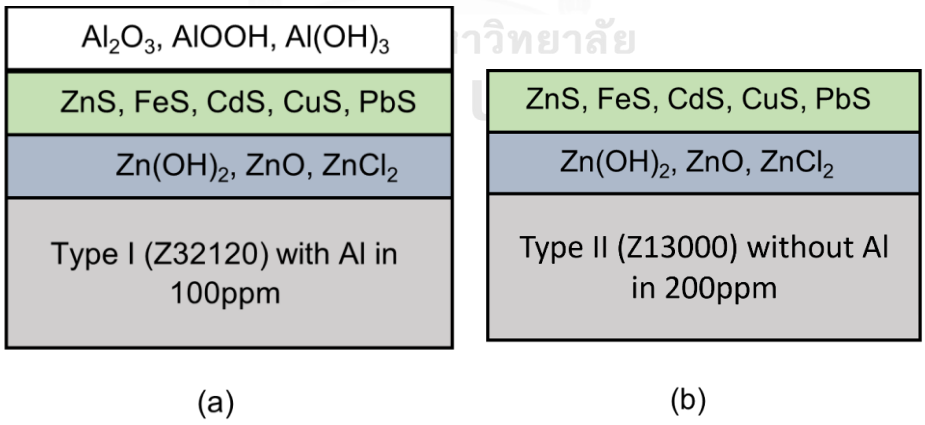

Figure 30-11. The schematic illustrations of sulfide layers formed by the $S_2O_3^{2-}$ concentration: a) Type 1 with Al in 100ppm, and b) Type 2 without Al in 200ppm

That is probably because $S_2O_3^{2-}$ greater than or equal to Cl^- concentration due to the high temperature at which pitting potential decreases. The more $S_2O_3^{2-}$, the thicker

sulfide layers growth blocking diffusive ions (OH^-, Cl^-) and denying Cl^- ion access into the surface sites where $S_2O_3^{2-}$ absorb into the surface oxygen vacancies [11, 20]. Also, the possible depletion of Cl^- increase $S_2O_3^{2-}$ concentration, probably by forming HCl which would be liberated as gas phase. Furthermore, the existence of SO_4^{2-} together with Cl^- can prevent the Cl^- corrosion or Cl^- penetrations since both ions compete to be absorbed on the surface. Due to the two negative charges of SO_4^{2-}, it has higher chance in nucleophilicity compared to Cl^-, thus greater SO_4^{2-} concentration will take the place of Cl^- on the surface as a result of Cl^- reduction which inhibits the film penetration and the film corrosion [41].

Therefore, for Type 1 (Zn32120), Al reacts with OH^- more than Cl^-, thereby creating $Al(OH)_3$ since Cl^- is not capable to get into the site to form $AlCl_3$. As in the case of Type 2 (Zn13000), it barely contains Al within, $S_2O_3^{2-}$ is likely to be increasingly oxidized to SO_4^{2-} which can impede the metal corrosion [35, 36]. Hence, if the immersion solution for Type 2 has higher concentration like 200ppm, there would be higher $S_2O_3^{2-}$ in the solution for the thicker sulfide layer growths.

Type 1 encounters this defect when it is immersed in 100ppm and Type 2 in 200ppm, all because of concentrations, immersion time and temperature. However, both alloys still can inhibit the passivation just by witnessing the slow decrease in current densities up to 720h at which the depassivation occurrence happened and proved by T. Kaewmaneekul et. al [1] .

4.3.6 Effect of thiosulfate with dissolve oxygen (DO)

The metal corrosion increases with the higher dissolved oxygen (DO) in the solution [35]. In the absence of thiosulfate, DO is draining in a rapid rate resulting the solution pH to be variable for acidity increasing with reacted sulfites [3]. The main role of $S_2O_3^{2-}$ is either increasing the oxygen scavenging rate or decreasing DO concentration, thereby to lead the impedance for corrosion or the breakdown of passive film in alkaline solution at elevated temperature [3, 35]. Also, DO increases the oxygen levels and corrosion rate.

Therefore, Type 2 (Zn13000) without Al, is suitable with less thiosulfate concentration since it does not have Al which would consume oxygen to create Al_2O_3 and later $AlCl_3$ for depassivation by Cl^- penetration. For Type 2, DO should be more so

that sulfide layers would not grow thicker to block the diffusive ions. As for Type 1 (Zn32120) with Al, it is better to have higher thiosulfate in the solution. Thus, DO is required more for Al to catch up for forming $AlCl_3$ via the formation of $Al(OH)_3$.

4.3.7 Limitation and Recommendation

This work has limitations over testing environments and parameters. In this work, the electrochemical tests were tested at 80°C after immersion times for 120h and 288hr at the same temperature. If the electrochemical tests are done at room temperature 25°C after immersion times at 80°C, the results are changed. This was witnessed by the errors of the first 3 rounds of experiments out of 8 rounds. The first 3 rounds were done without heating system during testing. The testing time has limitation over the surface area that expose to the testing solution according to the evaporation of the solution due to the heating effect Also, the oxidation can be happened on the counter electrode surface while the electrochemical tests are being conducted. That means that the counter electrode acts as an anode and the oxides from the working electrode become to attach on the surface of counter electrode. Therefore, the counter electrode is unable to use continuously for every electrochemical testing and it needs to be rinsed in 6% nitric acid at the end of each electrochemical testing to make the oxides to be spalled off.

Generally, the polarization curves turn out to have transpassive region after passivation. In this work, the tested results within the 1800s of testing time, were still in passive region and no transpassive region could be found. The short amount of testing time was not enough to reach the transpassive region in this work. However, by the slow and only slight changes in current density values within 1800s, the results of this work will be valid to inhibit the passivation even when the polarization test was longer. It is because the oxides on the samples have porous and poor adhesion due to the short circuit between cathode area and anode area of the working electrode. Also, there is slow nucleation that gives out poor grain boundaries on the surfaces leading to passive film breakdown. This breakdown can be witnessed by the dimension reduction of the final resulted samples after 288h as shown in Figure 4-12. Therefore, the passive current density values will not get to 5.6×10^{-6} A/cm^{-2}, which is the value of stable passive film, even at longer testing time.

For further research on this work, it is recommended to improve in testing samples dimensions to be longer in length exposing with the solution so that the testing time can be increased to investigate how long passive current density values will be greater than the passive film unstable value ($2x10^{-3}$ A/cm^{-2}) and clarify the current density at which transpassive region occurs. Moreover, either the 3-electrode cell should be advanced to double wall cell to contain the temperature at 80°C without heat loss that cause the ±2°C changes during the testing time or the heating system should be with the hotplate which can maintain constant 80°C.

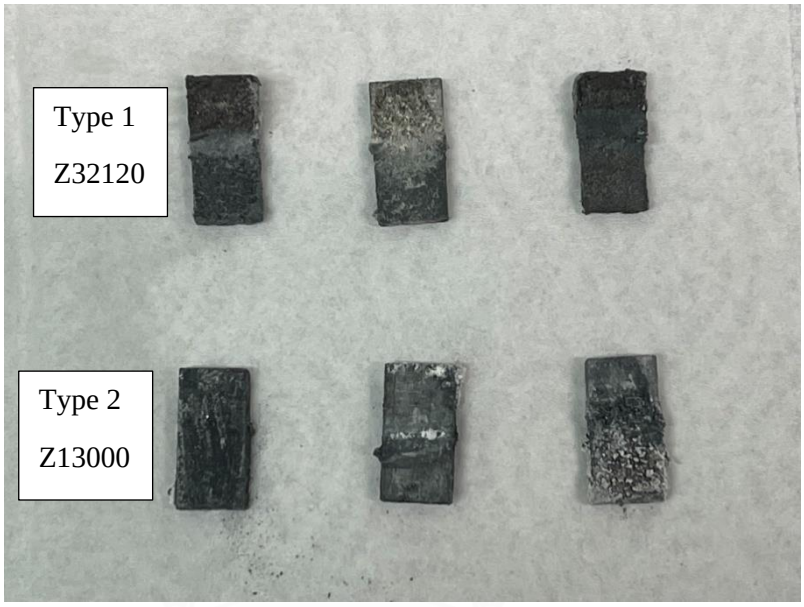

Figure 31-12. The final resulted samples of Type 1 (Z32120) and Type 2 (13000) after electrochemical test for 228h immersion time

CHAPTER (5)
CONCLUSION

5.1 Conclusion

The effect of thiosulfate on the passivation on the Zn-Al alloys in 3.5% NaCl solution at 80°C for 288h has been investigated by immersion tests, electrochemical tests, and FE-SEM observation. Summarily, the effect of thiosulfate can be described as follows:

1. Passivation on Type 1 (Z32120) with Al, and Type 2 (Zn13000) without Al can be inhibited between the immersion time of 120h and 288h.
2. Thiosulfate in Cl^- solution inhibits the passivation promoting the Cl^- penetration.
3. Cl^- penetration by Al content is more effective with thiosulfate existence.
4. Thiosulfate with Cl^- not only improves the hinderance of passivation on the metal but also it generates the depassivation if there are passive films and retards the repassivation.
5. The ratio of thiosulfate and Cl^- is important for passivation because the sulfide layers can grow thicker to block the diffusive species due to the higher concentration of thiosulfate.
6. Despite the impedance of passivation by all thiosulfate concentrations used in this work, the different thiosulfate concentrations give out different results based on immersion time and temperature.
7. For Type 1 (Z32120) with Al, the lower concentration of thiosulfate such as 100ppm, exhibits the decrease of current density at longer immersion time (288h) meanwhile higher thiosulfate concentrations (150ppm, 200ppm) increase in current density.
8. For Type 2 (Z13000) without Al, all thiosulfate concentrations increase the current densities, however, 100ppm and 200ppm were increased with half values less than 150ppm.
9. Since 100ppm and 200ppm give the controversial different effectiveness of thiosulfate and current density values depending on the time of immersion, 150ppm is the proper and average concentration which is free of this controversy for both Zn alloys, to be used in the solution.

APPENDIX

A. An example of polarization curve in NOVA software before setting up in Originlab

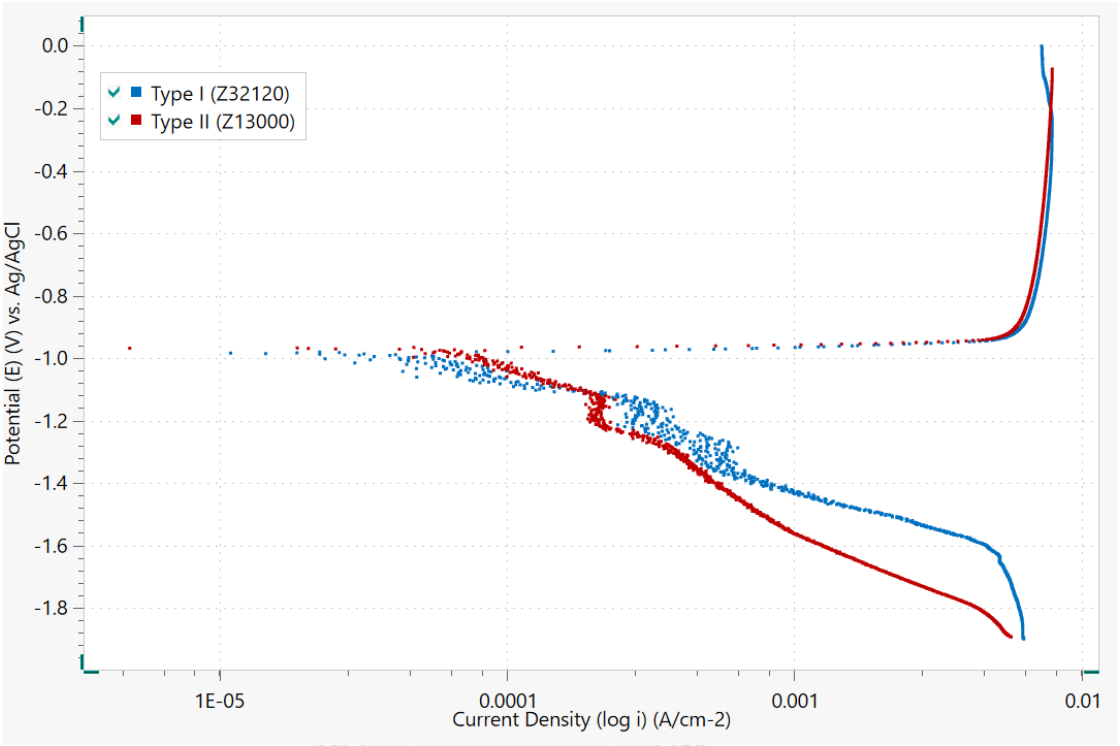

Polarization curves of Type 1 (Z32120) and Type 2 (13000) in 3.5%NaCl solution without thiosulfate

B. Potentiodynamic polarization curves of Type 1 (Z32120) and Type 2 (Z13000) tested for 7th round among 8 experiments

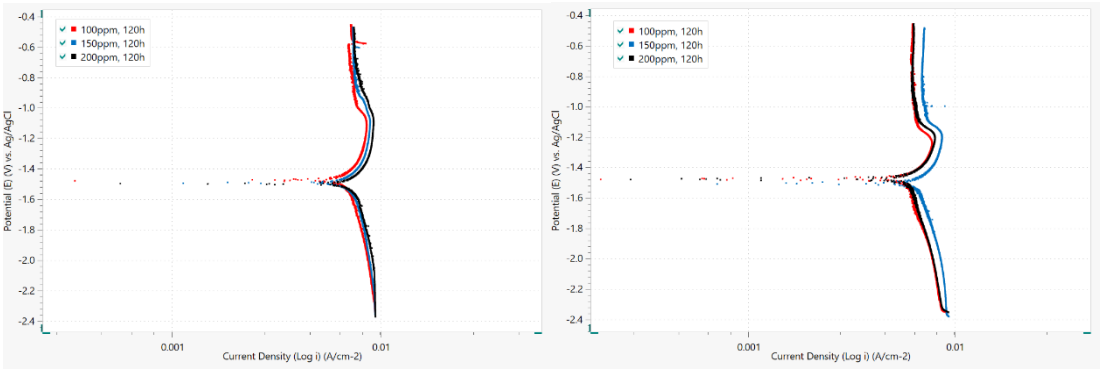

Polaization curves of Type 1 (Z32120) (left) and Type 2 (Z13000) (right) tested in 3.5%NaCl with thiosulfate (100ppm, 150ppm, 200ppm) after immersion of 120h

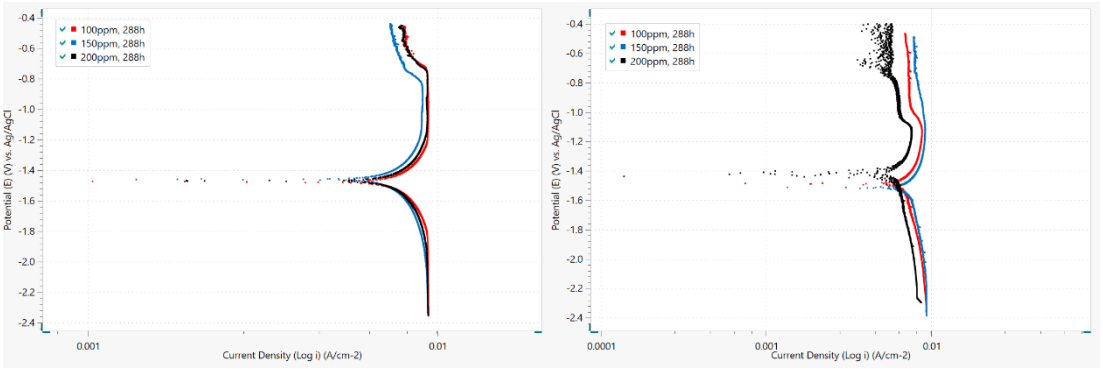

Polaization curves of Type 1 (Z32120) (left) and Type 2 (Z13000) (right) tested in 3.5%NaCl with thiosulfate (100ppm, 150ppm, 200ppm) after immersion of 288h

REFERENCES

[1] T. Kaewmaneekul and G. Lothongkum, "Effect of aluminium on the passivation of zinc–aluminium alloys in artificial seawater at 80 °C," *Corrosion Science*, vol. 66, pp. 67–77, 01/31 2013, doi: 10.1016/j.corsci.2012.09.004.

[2] B. Meyer, "Chapter 3 - Properties," in *Sulfur, Energy, and Environment*, B. Meyer Ed.: Elsevier, 1977, pp. 38-116.

[3] M. Cabrini, S. Lorenzi, and T. Pastore, "Effects of thiosulphates and sulphite ions on steel corrosion," *Corrosion Science*, vol. 135, pp. 158-166, 2018/05/01/ 2018, doi: https://doi.org/10.1016/j.corsci.2018.02.046.

[4] N. S. Al-Mamun, W. Haider, and I. Shabib, "Corrosion resistance of additively manufactured 316L stainless steel in chloride–thiosulfate environment," *Electrochimica Acta*, vol. 362, p. 137039, 2020/12/01/ 2020, doi: https://doi.org/10.1016/j.electacta.2020.137039.

[5] R. Walker, "Principles and prevention of corrosion: Denny A. Jones Macmillan, 1992, ISBN 0-02-361215-0, £16.95," *Materials & Design*, vol. 14, no. 3, p. 207, 1993/01/01/ 1993, doi: https://doi.org/10.1016/0261-3069(93)90066-5.

[6] B. N. Popov and S. P. Kumaraguru, "25 - Cathodic Protection of Pipelines," in *Handbook of Environmental Degradation of Materials (Second Edition)*, M. Kutz Ed. Oxford: William Andrew Publishing, 2012, pp. 771-798.

[7] B. N. Popov, "Chapter 15 - Cathodic Protection," in *Corrosion Engineering*, B. N. Popov Ed. Amsterdam: Elsevier, 2015, pp. 599-637.

[8] R. W. Evitts and G. F. Kennell, "Chapter 15 - Cathodic Protection," in *Handbook of Environmental Degradation of Materials (Third Edition)*, M. Kutz Ed.: William Andrew Publishing, 2018, pp. 301-321.

[9] B. N. Popov and J.-W. Lee, "Chapter 24 - Cathodic Protection of Pipelines," in *Handbook of Environmental Degradation of Materials (Third Edition)*, M. Kutz Ed.: William Andrew Publishing, 2018, pp. 509-532.

[10] R. F. Crundwell, "4.19 - Sacrificial Anodes," in *Shreir's Corrosion*, B. Cottis *et al.* Eds. Oxford: Elsevier, 2010, pp. 2763-2780.

[11] L. Choudhary, D. D. Macdonald, and A. Alfantazi, "Role of Thiosulfate in the Corrosion of Steels: A Review," *Corrosion*, vol. 71, no. 9, pp. 1147-1168, 2015, doi: 10.5006/1709.

[12] D. Zeng *et al.*, "Fracture failure analysis of the sacrificial anode protector in a water injection well," *Engineering Failure Analysis*, vol. 112, p. 104479, 2020/05/01/ 2020, doi: https://doi.org/10.1016/j.engfailanal.2020.104479.

[13] A. Bahadori, "2 - Application of Cathodic Protection," in *Cathodic Corrosion Protection Systems*, A. Bahadori Ed. Boston: Gulf Professional Publishing, 2014, pp. 35-89.

[14] V. Ashworth and D. Fairhurst, "The effect of temperature on the behaviour of a zinc-mild steel couple in a solution containing chloride ions," *Corrosion Science*, vol. 15, no. 6, pp. 669-686, 1975/01/01/ 1975, doi: https://doi.org/10.1016/0010-938X(75)90032-3.

[15] R. K. Ulrich, G. T. Rochelle, and R. E. Prada, "Enhanced oxygen absorption into bisulphite solutions containing transition metal ion catalysts," *Chemical Engineering Science*, vol. 41, no. 8, pp. 2183-2191, 1986/01/01/ 1986, doi: https://doi.org/10.1016/0009-2509(86)87134-2.

[16] J.-s. Mo, Z.-b. Wu, C.-j. Cheng, B.-h. Guan, and W.-r. Zhao, "Oxidation inhibition of sulfite in dual alkali flue gas desulfurization system," *Journal of Environmental Sciences*, vol. 19, no. 2, pp. 226-231, 2007/02/01/ 2007, doi: https://doi.org/10.1016/S1001-0742(07)60037-0.

[17] M. Kappes, G. S. Frankel, N. Sridhar, and R. M. Carranza, "Corrosion Behavior of Carbon Steel in Acidified, Thiosulfate-Containing Brines," *Corrosion*, vol. 68, no. 10, pp. 872-884, 2012, doi: 10.5006/0610.

[18] M. Kappes, G. Frankel, N. Sridhar, and R. Carranza, "Reaction Paths of Thiosulfate during Corrosion of Carbon Steel in Acidified Brines," *Journal of The Electrochemical Society*, vol. 159, p. C195, 01/01 2012, doi: 10.1149/2.085204jes.

[19] D. A. WENSLEY and R. S. CHARLTON, "Corrosion Studies in Kraft White Liquor: Potentiostatic Polarization of Mild Steel in Caustic Solutions Containing Sulfur Species," *Corrosion*, vol. 36, no. 8, pp. 385-389, 1980, doi: 10.5006/0010-9312-36.8.385.

[20] P. K. Baranwal and P. V. Rajaraman, "Electrochemical investigation on effect of sodium thiosulfate (Na2S2O3) and ammonium chloride (NH4Cl) on carbon steel corrosion," *Journal of Materials Research and Technology*, vol. 8, no. 1, pp. 1366-1378, 2019/01/01/ 2019, doi: https://doi.org/10.1016/j.jmrt.2018.05.029.

[21] Y. Zuo *et al.*, "Zinc dendrite growth and inhibition strategies," *Materials Today Energy*, vol. 20, p. 100692, 2021/06/01/ 2021, doi: https://doi.org/10.1016/j.mtener.2021.100692.

[22] R. Wahab, Y.-S. Kim, and H.-S. Shin, "Fabrication, characterization and growth mechanism of heterostructured zinc oxide nanostructures via solution method," *Current Applied Physics*, vol. 11, no. 3, pp. 334-340, 2011/05/01/ 2011, doi: https://doi.org/10.1016/j.cap.2010.07.030.

[23] A. Pola, M. Tocci, and F. E. Goodwin, "Review of Microstructures and Properties of Zinc Alloys," *Metals*, vol. 10, no. 2, p. 253, 2020. [Online]. Available: https://www.mdpi.com/2075-4701/10/2/253.

[24] G. Ramu, M. Lee, and H.-K. Jeong, "Effects of zinc salts on the microstructure and performance of zeolitic-imidazolate framework ZIF-8 membranes for propylene/propane separation," *Microporous and Mesoporous Materials*, vol. 259, pp. 155-162, 2018/03/15/ 2018, doi: https://doi.org/10.1016/j.micromeso.2017.10.010.

[25] X. Wang, J. Li, G. K. Das, S. Johanie, C. Vernon, and R. Shaw, "Characterization and crystal structure determination of zinc hydroxide chloride tetrahydrate Zn5(OH)8Cl2·4[(H2O)x(NH3)1−x]," *Journal of Solid State Chemistry*, vol. 290, p. 121483, 2020/10/01/ 2020, doi: https://doi.org/10.1016/j.jssc.2020.121483.

[26] J. G. Speight, "2 - The properties of water," in *Natural Water Remediation*, J. G. Speight Ed.: Butterworth-Heinemann, 2020, pp. 53-89.

[27] T. M. Seward, A. E. Williams-Jones, and A. A. Migdisov, "13.2 - The Chemistry of Metal Transport and Deposition by Ore-Forming Hydrothermal Fluids," in *Treatise on Geochemistry (Second Edition)*, H. D. Holland and K. K. Turekian Eds. Oxford: Elsevier, 2014, pp. 29-57.

[28] N. S. Bolan and K. Kandaswamy, "pH," in *Encyclopedia of Soils in the Environment*, D. Hillel Ed. Oxford: Elsevier, 2005, pp. 196-202.

[29] F. H. Stephenson, "Chapter 2 - Solutions, Mixtures, and Media," in *Calculations for Molecular Biology and Biotechnology (Third Edition)*, F. H. Stephenson Ed. Boston: Academic Press, 2016, pp. 15-42.

[30] A. Król, K. Mizerna, and M. Bożym, "An assessment of pH-dependent release and mobility of heavy metals from metallurgical slag," *Journal of Hazardous Materials*, vol. 384, p. 121502, 2020/02/15/ 2020, doi: https://doi.org/10.1016/j.jhazmat.2019.121502.

[31] T. M. Bawazeer, A. M. E. Defrawy, and A. A. El-Shafei, "Corrosion inhibition of zinc in sodium sulphate solution using nonionic surfactants of tween series: Experimental and theoretical study," *Colloids and Surfaces A: Physicochemical and Engineering Aspects*, vol. 520, pp. 694-700, 2017/05/05/ 2017, doi: https://doi.org/10.1016/j.colsurfa.2017.02.025.

[32] T. Ben Nasr, N. Kamoun, M. Kanzari, and R. Bennaceur, "Effect of pH on the properties of ZnS thin films grown by chemical bath deposition," *Thin Solid Films*, vol. 500, no. 1, pp. 4-8, 2006/04/03/ 2006, doi: https://doi.org/10.1016/j.tsf.2005.11.030.

[33] B. W. Sanders and A. H. Kitai, "The electrodeposition of thin film zinc sulphide from thiosulphate solution," *Journal of Crystal Growth*, vol. 100, no. 3, pp. 405-410, 1990/03/01/ 1990, doi: https://doi.org/10.1016/0022-0248(90)90238-G.

[34] D. Domyati, "Chemical and thermal study of metal chalcogenides (zinc sulfide), aluminum oxide, and graphene oxide based nanocomposites for wastewater treatment," *Ceramics International*, 2022/09/22/ 2022, doi: https://doi.org/10.1016/j.ceramint.2022.09.190.

[35] F. Ning *et al.*, "Effects of thiosulfate and dissolved oxygen on crevice corrosion of Alloy 690 in high-temperature chloride solution," *Journal of Materials Science & Technology*, vol. 66, pp. 163-176, 2021/03/10/ 2021, doi: https://doi.org/10.1016/j.jmst.2020.05.074.

[36] P. L. F. van den Bosch, D. Y. Sorokin, C. J. N. Buisman, and A. J. H. Janssen, "The Effect of pH on Thiosulfate Formation in a Biotechnological Process for the Removal of Hydrogen Sulfide from Gas Streams," *Environmental Science & Technology*, vol. 42, no. 7, pp. 2637-2642, 2008/04/01 2008, doi: 10.1021/es7024438.

[37] M. Zakeri, M. Naghizadeh, D. Nakhaie, and M. H. Moayed, "Pit Transition Potential and Repassivation Potential of Stainless Steel in Thiosulfate Solution," *Journal of The Electrochemical Society*, vol. 163, pp. C275-C281, 01/01 2016, doi: 10.1149/2.0381606jes.

[38] T. Lange *et al.*, "Alumina-Protected, Durable and Photostable Zinc Sulfide Particles from Scalable Atomic Layer Deposition," *Advanced Functional Materials*, vol. 31, no. 14, p. 2009323, 2021, doi: https://doi.org/10.1002/adfm.202009323.

[39] A. Farooq, M. Hamza, Q. Ahmed, and K. M. Deen, "Evaluating the performance of zinc and aluminum sacrificial anodes in artificial seawater," *Electrochimica Acta*, vol. 314, pp. 135-141, 2019/08/10/ 2019, doi: https://doi.org/10.1016/j.electacta.2019.05.067.

[40] J. P. Calderón *et al.*, "Corrosion Behavior of Al Modified with Zn in Chloride Solution," *Materials*, vol. 15, no. 12, p. 4229, 2022. [Online]. Available: https://www.mdpi.com/1996-1944/15/12/4229.

[41] C. Chen, L. Jiang, M.-Z. Guo, P. Xu, L. Chen, and J. Zha, "Effect of sulfate ions on corrosion of reinforced steel treated by DNA corrosion inhibitor in simulated concrete pore solution," *Construction and Building Materials*, vol. 228, p. 116752, 2019/12/20/ 2019, doi: https://doi.org/10.1016/j.conbuildmat.2019.116752.

VITA

NAME	Thwelt Thinzar Zaw
DATE OF BIRTH	20 October 1995
PLACE OF BIRTH	Mandalay, Myanmar
INSTITUTIONS ATTENDED	University of Technology (Yatanarpon Cyber City)
HOME ADDRESS	No.181/33A, 74 Road, between 32 & 33 Streets, Chanayetharzan Township, Mandalay, Myanmar
PUBLICATION	Effect of thiosulfate on the passivation of zinc-alloys in 3.5 wt% NaCl solution at 353K Material Testing 65 (2023) 5, pages 715-724, DOI 10.1515/mt-2022-0399
AWARD RECEIVED	ASEAN or NON-ASEAN scholarship award by Chulalongkorn University